Universidade de Aveiro

Ano 2021

Rui Pedro Nóbrega Chanoca

Técnicas de Igualização Adaptativas com Estimativas Imperfeitas do Canal para os Futuros Sistemas 5G

Adaptive Equalization Techniques with Imperfect Channel Estimates for Future 5G Systems

2021

Universidade de Aveiro

Ano 2021

Rui Pedro Nóbrega Chanoca

Técnicas de Igualização Adaptativas com Estimativas Imperfeitas do Canal para os Futuros Sistemas 5G

Adaptive Equalization Techniques with Imperfect Channel Estimates for Future 5G Systems

Dissertação apresentada à Universidade de Aveiro para cumprimento dos requisitos necessários à obtenção do grau de Mestre em Engenharia Eletrónica e Telecomunicações, realizada sob a orientação científica do Professor Doutor Adão Silva (orientador), Professor auxiliar do Departamento de Eletrónica, Telecomunicações e Informática da Universidade de Aveiro e do Doutor Pedro Pedrosa (co-orientador), investigador no Instituto de Telecomunicações de Aveiro.

This work is supported by the European Regional Development Fund (FEDER), through the Competitiveness and Internationalization Operational Program (COMPETE 2020) of the Portugal 2020 framework, Regional OP Centro (CENTRO 2020), Regional OP Lisboa (LISBOA 14-20) and by FCT/MEC through national funds, under Project MASSIVE5G (AAC no 02/SAICT/2017)"

o júri

presidente	Prof. Doutor Pedro Miguel da Silva Cabral professor auxiliar, Universidade de Aveiro
arguente principal	Prof. Doutor Rui Miguel Henriques Dias Morgado Dinis professor associado com agregação, Universidade Nova de Lisboa
orientador	Prof. Doutor Adão Paulo Soares Silva professor associado, Universidade de Aveiro

Agradecimentos

Ao longo do desenvolvimento desta dissertação eu recebi enorme suporte e assistência de vários intervenientes.

Gostaria assim de expressar a minha sincera gratidão aos meus orientadores, Prof. Adão Paulo Soares da Silva e Prof. Pedro Miguel Ferreira de Oliveira Pedrosa, pelo seu apoio indispensável e pela continua disponibilidade fornecida ao longo deste último ano tumultuoso.

Gostaria de agradecer à minha família pelo seu suporte continuo aos meus estudos.

E finalmente gostaria de agradecer à Universidade de Aveiro, ao Departamento de Eletrónica, Telecomunicações e Informática e ao Instituto de Telecomunicações por disponibilizarem as necessárias condições para o meu desenvolvimento académico e subsequentemente o desenvolvimento desta dissertação.

Palavras-chave OFDM, OFDMA, SC-FDMA, MIMO, IB-DFE

Resumo

Redes sem fios têm crescido de maneira contínua e exponencial desde a sua incepção. A tremenda exigência para altas taxas de dados e o suporte para um elevado número de utilizadores sem aumentar a interferência disruptiva originada por estes são alguns dos focos que levaram ao desenvolvimento de técnicas de compensação e novas tecnologias.

"Orthogonal frequency division multiplexing" (OFDM) é um dos exemplos de tecnologias que se destacaram nesta última década, visto ter fornecido uma plataforma para transmissão de dados sem-fio eficaz e simples.

O seu maior problema é a alta "peak-to-average power ratio" (PAPR) e a sua sensibilidade a ruído de fase que deram motivo à adoção de técnicas alternativas, tais como os sistemas "single carrier" com "frequency domain equalization" (SC-FDE) ou os sistemas "multi-carrier" com "code division multiple access" (MC-CDMA), mas equalizadores não lineares no domínio de frequência têm sido alvo de especial atenção devido ao seu melhor desempenho. Destes, o "iterative block decision feedback equalizer" (IB-DFE) tem-se provado especialmente promissor devido à sua compatibilidade com técnicas de diversidade no espaço, sistemas MIMO e esquemas CDMA.

No entanto, IB-DFE requer que o sistema tenha constante conhecimento das propriedades dos canais usados, ou seja, necessita de ter perfeito "channel state information" (CSI) constantemente, o que é tanto irrealista como impossível de implementar.

Nesta dissertação iremos projetar um recetor IB-DFE alterado de forma a conseguir detetar sinais dum transmissor baseado em tecnologia SC-FDMA, mesmo com a informação de estado de canal errada. Os resultados irão então demonstrar que o novo esquema de equalização proposto é robusto para situações de CSI imperfeito (I-CSI), visto que o seu desempenho se mantém próximo dos valores esperados para CSI perfeito, em apenas algumas iterações.

Keywords OFDM, OFDMA, SC-FDMA, MIMO, IB-DFE

Abstract

Wireless communication networks have been continuously experiencing an exponential growth since their inception. The overwhelming demand for high data rates, support of a large number of users while mitigating disruptive interference are the constant research focus and it has led to the creation of new technologies and efficient techniques.

Orthogonal frequency division multiplexing (OFDM) is the most common example of a technology that has come to the fore in this past decade as it provided a simple and generally ideal platform for wireless data transmission.
It's drawback of a rather high peak-to-average power ratio (PAPR) and sensitivity to phase noise, which in turn led to the adoption of alternative techniques, such as the single carrier systems with frequency domain equalization (SC-FDE) or the multi carrier systems with code division multiple access (MC-CDMA), but the nonlinear Frequency Domain Equalizers (FDE) have been of special note due to their improved performance. From these, the Iterative Block Decision Feedback Equalizer (IB-DFE) has proven itself especially promising due to its compatibility with space diversity, MIMO systems and CDMA schemes.

However, the IB-DFE requires the system to have constant knowledge of the communication channel properties, that is, to have constantly perfect Channel State Information (CSI), which is both unrealistic and impractical to implement.

In this dissertation we shall design an altered IB-DFE receiver that is able to properly detect signals from SC-FDMA based transmitters, even with constantly erroneous channel states. The results shall demonstrate that the proposed equalization scheme is robust to imperfect CSI (I-CSI) situations, since its performance is constantly close to the perfect CSI case, within just a few iterations.

Index

List of Figures

List of Tables

List of Acronyms

Acronyms	Meaning
1G	First Generation
2G	Second Generation
3G	Third Generation
4G	Second Generation
5G	Fifth Generation
8-PSK	8-Phase Shift Keying
ADC	Analog to Digital Converter
AMPS	Analogue Mobile Phone System
BER	Bit Error Rate
BS	Base Station
CDMA	Code Division Multiple Access
CP	Cyclic Prefix
CS	Circuit Switching
CSI	Channel State Information
D-AMPS	Digital Advanced Phone System
DAC	Digital to Analogue Converter
DFE	Decision Feedback Equalization
DFT	Discrete Fourier Transform
EDGE	Enhanced Data for Global Evolution
eMBB	Enhanced Mobile Broadband
EVDO	Evolution Data Optimized
FBMC	Filter Bank Multicarrier
FDD	Frequency Division Duplex
FDE	Frequency Domain Equalization
FDM	Frequency Division Multiplexing
FFT	Fast Fourier Transform
GFDM	Generalized Frequency Division Multiplexing
GMSK	Gaussian Minimum-Shift Keying
GRPS	General Packet Radio Services

GSM	Global System for Mobile communication
HSPA	High-Speed Packet Access
IB-DFE	Iterative Block Decision Feedback Equalization
ICI	Inter-Carrier Interference
I-CSI	Imperfect Channel State Information
IDFT	Inverse Discrete Fourier Transform
IFFT	Inverse Fast Fourier Transform
IS-95	Interim Standard 95
ISI	Inter Symbol Interference
KKT	Karush-Kuhn-Tucker
LAN	Local Area Network
LLRs	Log Likelihood Ratios
LTE	Long Term Evolution
LTE-A	Long Term Evolution Advanced
M2M	Machine to Machine
MFB	Matched Filter Bound
MIMO	Multiple Input Multiple Output
MISO	Multiple Input Single Output
MMS	Multimedia Messaging Service
MMSE	Minimum Mean Square Error
MSE	Mean Square Error
mMTC	Massive Machine Type Communication
mMIMO	Massive MIMO
NFV	Network Function Virtualization
NMT	Nordic Mobile Telephone
NR	New Radio
OFDM	Orthogonal Frequency Division Multiplexing
OFDMA	Otrhogonal Frequency Division Multiple Access
PA	Power Amplifier
PAPR	Peak-to-Average Power Ratio
PIC	Parallel Interference Cancellation
PS	Packet Switching
QAM	Quadrature Amplitude Modulation
QPSK	Quadrature Phase Shift Keying

SC	Single Carrier
SC-FDE	Single Carrier Frequency Domain Equalization
SC-FDMA	Single Carrier Frequency Division Multiple Access
SDN	Software Define Networking
SIC	Successive Interference Cancellation
SIMO	Single Input Multiple Output
SINR	Signal-to-Interference plus Noise Ratio
SISO	Single Input Single Output
SMS	Short Message Services
STBC	Space-Time Block Coding
STC	Space-Time Coding
SU-MIMO	Single User MIMO
TACS	Total Access Communication System
TDD	Time Division Duplex
TDMA	Time Division Multiple Access
UE	User Equipment
UFMC	Universal Filtered Multi-Carrier
UMTS	Universal Mobile Telecommunication Systems
URLLC	Ultra-Reliable Low Latency Communication
WCDMA	Wideband CDMA
WLAN	Wireless LAN
ZF	Zero-Forcing

1. Introduction

1.1 Mobile Network Evolution

The first generation of mobile telecommunication systems (1G) started in the 1970s with the development of various analogue systems, such as the Analogue Mobile Phone System (AMPS), Nordic Mobile Telephone (NMT), C450, Nippon Telegraph and Telephone (NTT), and Total Access Communication Access (TACS). These analogue systems were expensive, bulky and had inefficient spectral utilization.

The second generation system (2G) started the digital era of mobile communications. The use of digital voice codification and modulation techniques introduced the implementation of new access technologies like Time Division Multiple Access (TDMA) and Code Division Multiple Access (CDMA), which enabled highly secure voice and text messaging services, as well as limited data services, to multiple users.

The most important of these second generation systems was GSM (originally Groupe Special Mobile and now Global System for Mobile communication) which was launched in 1991 in Finland. Even though GSM was not created with data services in mind it did introduce mobile data services, starting with the short message services (SMS) and later with Multimedia Messaging Service (MMS) [1]. The starting data rates were around 14.4 kbit/s and reached values up to 64 kbit/s. The cell horizontal radius, while varying depending on antenna height, gain and propagation conditions, was able to support in practical use 35 kilometers. GSM usage of Gaussian Minimum-Shift Keying modulation (GMSK) and Frequency Division Duplex (FDD), meaning that the signal is first smoothed with a Gaussian low-pass filter and then fed to a frequency modulator, greatly reducing the adjacent channel interference.

Digital Advanced Phone System (D-AMPS) and Interim Standard 95 (IS-95) were the other technologies used when launching second-generation mobile networks. For better data transmission the GSM was improved through the usage of Packet Switching (PS) instead of

simple Circuit Switching (CS) led to an increase of data rates to 114 Kbit/s and the creation of the General Packet Radio Services (GRPS). The ever constant need for better rates of data transmission brought forth by mobile internet connections led to the creation of the Enhanced Data for Global Evolution (EDGE) systems that use 8-Phase Shift Keying (8-PSK) and reaches up to 384 Kbit/s by coding 3 bits per symbol.

The third generation of mobile networks (3G) were split into two systems based on CDMA technology. The first was the Universal Mobile Telecommunication Systems (UMTS) and the other was CDMA2000. UMTS was used for migrating GSM networks to 3G while CDMA2000 was the equivalent for IS-95 and D-AMPS [2].

UMTS employs Wideband CDMA (WCDMA) for its access and offers peak downlink speeds of up to 2 Mbit/s. These networks were further enhanced through a technology called High-Speed Packet Access (HSPA), which offered peak downlink and uplink speeds of up to 14.4 Mbit/s and 5.76 Mbits respectively. Later an Evolved version of the technology known as HSPA+ was introduced, providing data rates of up to 42 Mbit/s in the downlink and 11.5 Mbit/s in the uplink. CMDA2000 was able to support up to 153 Kbit/s in both downlink and uplink. These data rates were further enhanced through the Evolution Data Optimized (EVDO) technology to reach up to 14.7 Mbit/s in downlink and 5.4 Mbit/s in the uplink.

In the 2010s 3GPP started to work on the fourth generation (4G) of mobile systems with the Long Term Evolution technology (LTE), colloquially known as 3.9G, that was further refined into LTE-Advanced (LTE-A), with peak data rates of 1Gbit/s in the uplink and 500 Mbit/s in the downlink, which became the standard 4G LTE technology [3]. These were created with the purposes of not only continuing to achieve higher data rates, but also decreasing the signal latency and increasing bandwidth efficiency. LTE uses Multiple Input Multiple Output (MIMO) systems to increase the overall bitrate through multiplexing, that is, transmitting various data streams through multiple different antennas using the same resources in both frequency and time, together with multiple access schemes known as Orthogonal Frequency Division Multiple Access (OFDMA) in its downlink and Single Carrier Frequency Division Multiple Access (SC-FDMA) in its uplink. These multiple access schemes provide orthogonality between users, which consequently reduces the interference and increase the network capacity. [4]

1.2 5th Generation

The tremendous growth of the number of connected devices, the substantial increase in network traffic volume, and the increasingly wide range of applications with varying requirements and characteristics, have motivated industry efforts and investment toward defining, developing, and deploying systems for the fifth generation (5G) of mobile networks. To meet these emerging diverse service requirements, the fifth generation of mobile networks developed by 3GPP, known as 5G NR (New Radio), has divided them into three different sets, one for each service, namely, enhanced mobile broadband (eMBB), ultra-reliable low latency communication (URLLC), and massive machine type communication (mMTC). eMBB focuses on very high data rate and large bandwidth requirements, URLLC requires very low latency, very high reliability, and availability, while mMTC needs low bandwidth, high connection density, enhanced coverage, and low energy consumption at the user end [5] [6]. These services' spectrum usage can vary from sub-1 GHz to 100GHz, making them rather incompatible with LTE systems.

To fulfill these diverse services' requirements, the use of several new waveforms and multiple access schemes, such as filter bank multi-carrier (FBMC), generalized frequency division multiplexing (GFDM), and universal filtered multi-carrier (UFMC), were pondered. However, while each of these considered schemes have shown improvements over OFDM, their complexity, practical limitations, and OFDM's already established standardization has led the 3GPP community to adopt the OFDM waveform with adaptive numerology as 5G NR's basic signal format. This allows configurable frame structures and radio resource allocations depending on the, available spectrum, and bandwidth without affecting backward compatibility with legacy LTE systems [7].

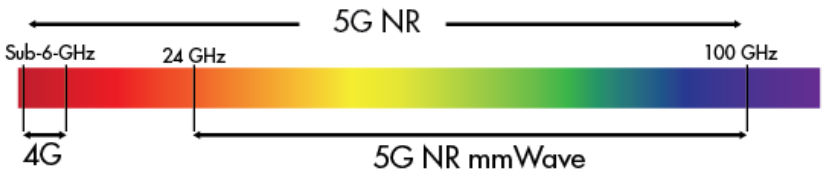

Figure 1 - 5G Spectrum Usage [8]

Due to the high propagation loss of the employed high frequency waveforms, known as millimeter waves (mmWaves), and the users' high bandwidth demands, beamforming techniques became a critical piece of 5G NR to increase spectral efficiency while providing reliable coverage [8]. The basic idea behind beamforming is to optimally transmit signals from transmitters with multiple antennas while maximizing each user's received signal and

minimizing the interference from other users, increasing capacity. This can be done by transmitting the same signal from all antennas with different amplitudes and phases in such a way that the they form a strong beam towards the direction of the desired terminal and cancelling beams of interfering signals.

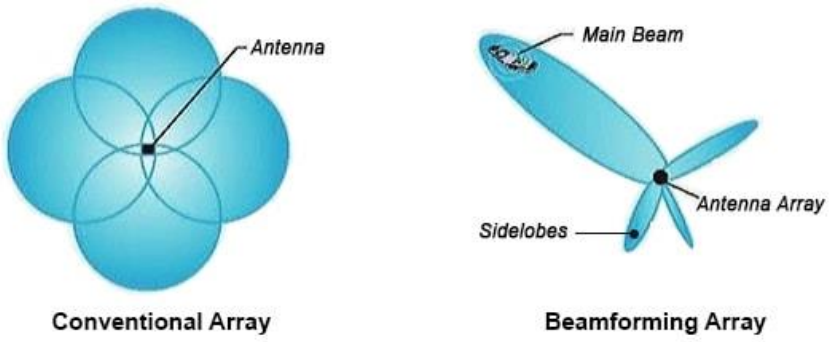

Figure 2 - Conventional Array & Beamforming Array Comparison [9]

The performance of 5G NR technology is further increased by applying the beamforming technique onto massive MIMO (mMIMO) systems. These mMIMO systems are MIMO systems wherein the transmitters and/or receivers contain numerous antennas. Such a large number of antennas can improve the energy efficiency by approximately 100-fold and the capacity of wireless communication systems 10-fold, reaching peak data rates of 20 Gbit/s in the uplink and 10 Gbit/s in the downlink. The interference issues derived from using such high number of antennas are then mitigated with the use of beamforming [6].

.

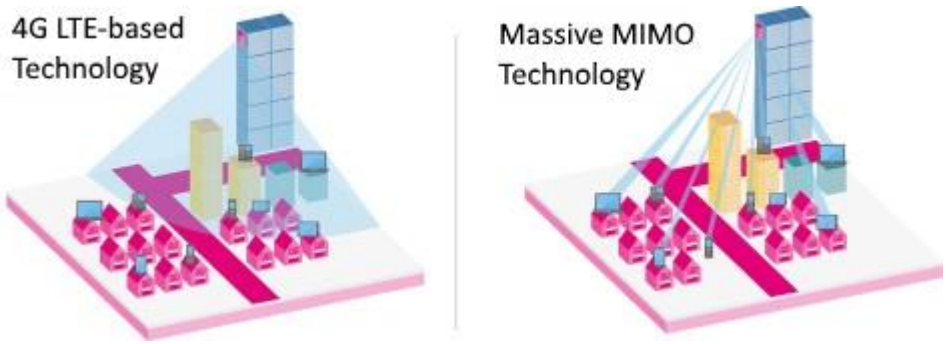

Figure 3 - 4G's LTE & 5G's Massive MIMO scheme mock-up [10]

To achieve the preceding techniques and overcome the challenges defined for 5G networks, there is a need for new, more flexible, and versatile, network architecture designs, such as Software-Defined Networking (SDN) and Network Function Virtualization (NFV). The SDN architecture segregates the network control functions from network forward functions, enabling the network control to become directly programmable, centrally

manageable and makes it easier to extend the network with new functionality. While NFV is a network architecture that virtualizes network services that were traditionally run on hardware into packaged virtual machines, which improves scalability and agility as it allows network services and applications to be applied on demand without requiring additional hardware resources. Superimposing these two architectures simultaneously allows more flexible virtualized networks that uses resources efficiently and can be centrally programmable [11] [12].

1.3 Motivation and Objectives

The explosion of the number of mobile subscriptions and connected devices as well as the associated data volume is expected to continue its exponential growth trend. As can be seen in the Fig. 4 and Fig. 5, it is predicted that in 2023, 9.8 billion mobile subscriptions and 29.3 billion connected devices are expected. Furthermore, the data-traffic is expected to continue its past trend of doubling every year (1000 times in 10 years) [13] [14] [15]. Therefore, new technologies and more efficient algorithm designs are needed.

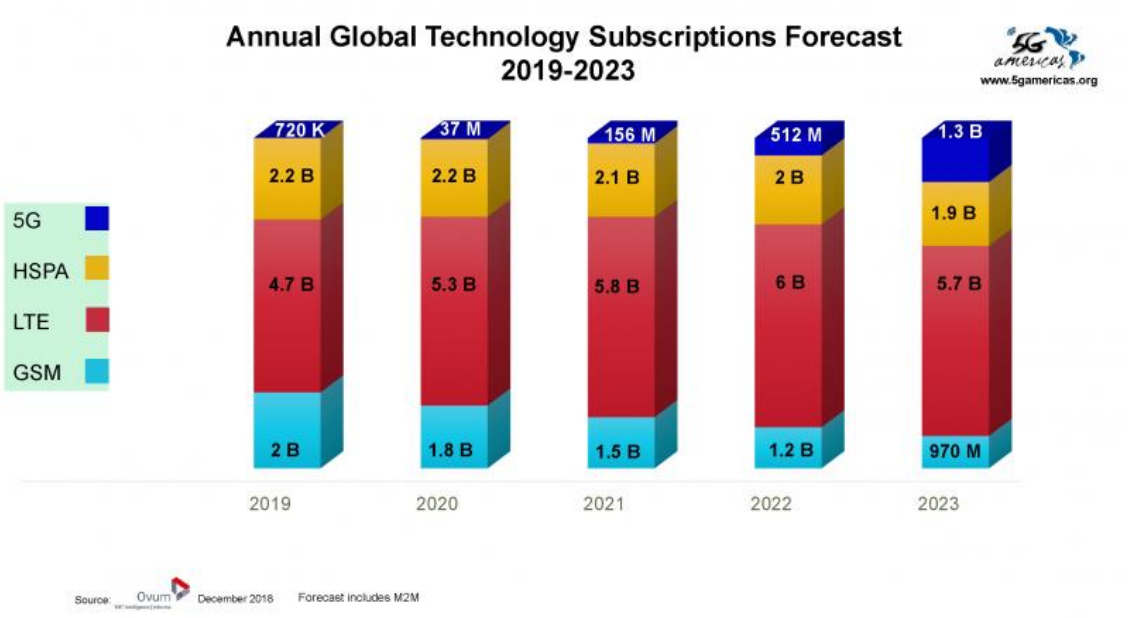

Figure 4 - Annual Global Technology Subscriptions Forecast 2019-2023 [16]

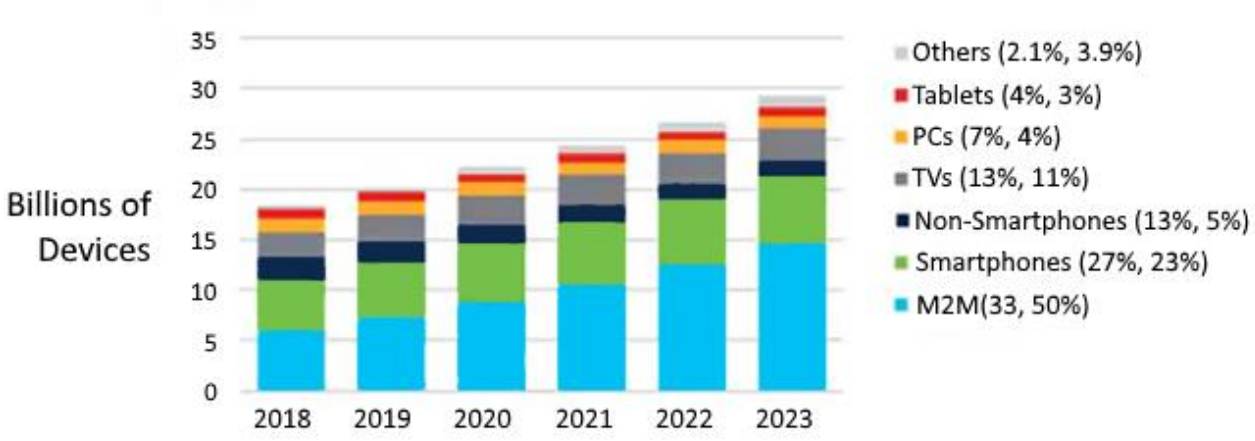

Figure 5 - Annual Global User Devices Forecast 2018-2023 [14]

Orthogonal frequency division multiplexing (OFDM) is a simple, and well-accepted technique to mitigate the effects of inter-symbol interference in frequency selective channels [17]. Combining OFDM with multiple-input multiple-output (MIMO), producing so called MIMO-OFDM, significantly reduces receiver complexity in wireless broadband systems, thus making it a competitive choice for broadband wireless communication systems, and has already been adopted in some high rate wireless communications standards such as Wi-Fi, 4G and in the recent 5G, namely for the downlink [18] [19]. The main drawback of OFDM modulations are the high signal fluctuations that lead to large peak-to-average power ratio (PAPR) [20]. This causes some challenges to the power amplifier (PA) design since OFDM is sensitive to nonlinear distortions caused by PA [21]. The amplifier must stay in the linear area with the use of extra power backoff, in order to prevent problems to the output signal.

To overcome this drawback single-carrier frequency-division multiple access (SC-FDMA), a modified form of orthogonal frequency-division multiple access (OFDMA), was proposed as an alternative for the uplink. When compared with OFDM\A, SC-FDMA has similar throughput and essentially the same overall complexity. A principal advantage of SC-FDMA is the peak-to average power ratio (PAPR) [22], which is lower than that of OFDM. SC-FDMA was adopted for the uplink, as a multiple access scheme, of the long-term evolution (LTE) cellular system [23]. For the 5G uplink it adopted another Single Carrier (SC) based scheme, the discrete Fourier transform spread orthogonal frequency division multiplexing (DFT-s-OFDM) scheme [24] which is quite similar to SC-FDMA.

However, the residual interference levels of these SC based systems might still be too high [25], leading to performance that is still several dB from the Matched Filter Bound (MFB). To solve this issue, nonlinear decision feedback equalization (DFE) schemes have been proposed, with the Iterative-Block Decision Feedback Equalization (IB-DFE) being the

most promising nonlinear FDE technique, which was originally proposed in [26] and was extended for a wide range of scenarios in the last years, ranging from diversity scenarios, multiplexing MIMO and MC-CDMA systems, among many others.

However, most of the previous IB-DFE based schemes assume perfect channel state information (CSI), which is not realistic for practical implementations where the channel faces some errors. Therefore, this work intends to fill some of the gap and design an IB-DFE algorithm that explicitly takes into account the channel errors. The main objective of this work is to extend the IB-DFE scheme designed to SC-FDMA systems and perfect CSI [27] to the practical case where the channel has errors.

1.4 Outline

After the overview of the evolution of mobile networks, the motivation and objectives of this dissertation, we will continue with following chapters:

In the second chapter, the most standard multi-access schemes used in network communications, OFDM and SC-FDMA, are presented and studied.

In the third chapter we explore the diversity and multiplexing techniques present in MIMO systems alongside multi-user linear and iterative equalization schemes.

The fourth chapter deals with the main components of this thesis. The implemented system is presented, with the block structure of the transmitter and receiver being detailed and their mathematical steps detailed. The outcome that the system has produced is then shown and studied.

Lastly, the fifth chapter states the conclusion of the dissertation while making recommendations for future work on the topic.

2. Multiple-Access Schemes

In modern mobile communication systems, schemes that enable several users to gain access to both uplink and downlink simultaneously has become a necessity. As such, various robust multiple-access schemes have been developed in order to ensure an efficient transmission and equalization of the received signals.

2.1 OFDM

Orthogonal Frequency Division Multiplexing is a Frequency Division Multiplexing (FDM) scheme based on multiple overlapping orthogonal subcarrier signals transmitted in parallel, each with a Cyclic Prefix (CP) or Guard Interval, to eliminate Inter Symbol Interference (ISI) [28].

As a communication system with multi-carrier modulation, it transmits N_c complex-valued symbols S_n, $n = 0 \dots, N_c - 1$, in parallel N_c sub-carriers. The source symbol duration T_d results after serial-to-parallel conversion in the OFDM symbol duration

$$T_s = N_c T_d \tag{2.1}$$

OFDM's high spectral efficiency, easy implementation and robustness against narrow-band and inter symbol interference has led it to be implemented in various Wireless LAN (WLAN) interfaces, digital radio systems and visual distribution systems.

- **Orthogonality**

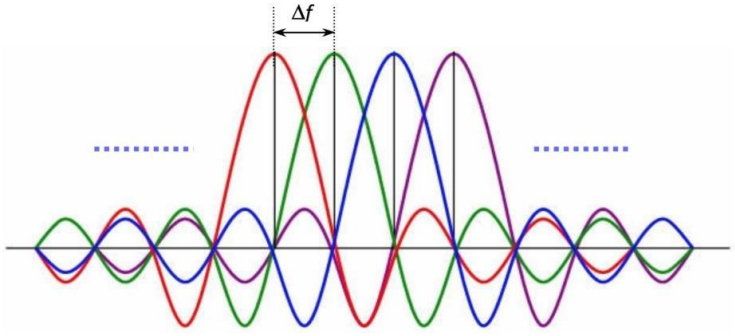

Figure 6 - Demonstration of Orthogonality in the OFDM [29]

All OFDM subcarriers must be orthogonal with each other. This implies that the following criteria is followed:

$$\int_{T}^{(n+1)T} x_1(t)x_2(t)dt = 0 \quad (2.2)$$

With $x_1(t)$ and $x_2(t)$ representing the signals in the time domain within the subcarriers. This allows the transmission of multiple subcarriers at the same time, increasing the efficiency of the bandwidth usage, without any inter-signal interference.

- **Cyclic Prefix**

When OFDM signals are being transmitted in multipath fading channels, various copies of the transmitter signal can be received at slightly different time intervals, which can cause ISI and possibly even losing the signal's orthogonality, causing additional ICI as well. To fix this issue a Cyclic Prefix is to be implemented, that is, a copy of the end portion of the OFDM symbol is put in its beginning as a guard interval.

To completely avoid ISI and maintain orthogonality between the sub-carriers to avoid ICI, the Cyclic Prefix duration, T_G must naturally be greater than the delay spread of the channel, τ_{max}, but this Cyclic Prefix brings with it a loss in spectral efficiency, as it reduces the transmission rate. Taking this into account, the Cyclic Prefix is established to never be greater than a quarter of the OFDM symbol's duration, T_{OFDM}.

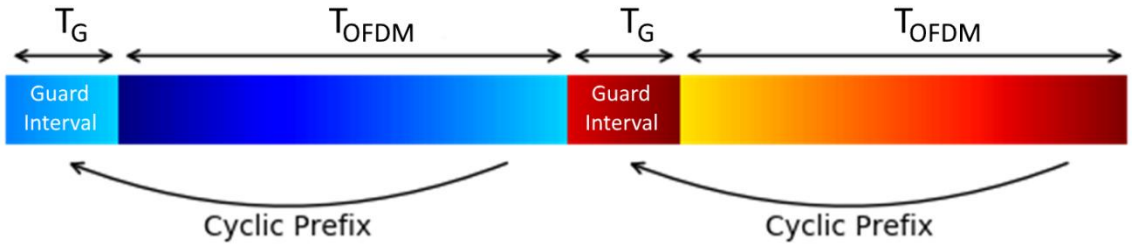

Figure 7 - Cyclic Prefix [30]

The specific duration of T_G used depends on the overall subcarrier spacing, Δf, used. In LTE technologies, it is established as only 15kHz, while in 5G NR five types of subcarrier spacing are used, as can be seen in Table 1. [31]

μ	$\Delta f = 2^{\mu} \cdot 15$[kHz]	T_G [μs]	T_{OFDM} [μs]
0	15	4.69	66.67
1	30	2.34	33.33
2	60	1.17	16.67
3	120	0.57	8.33
4	240	0.29	4.17

Table 1 - OFDM Symbol Duration for 5G NR

- **OFDM Block Diagram**

An OFDM system can be implemented through the combination of the different blocks as shown in Fig.8:

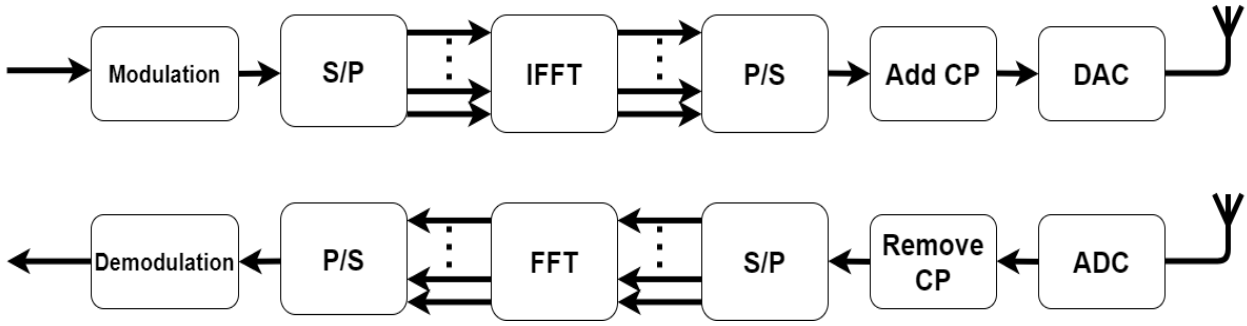

Figure 8 - OFDM Block Diagram

When transmitting an OFDM signal, first the Serial to Parallel block converts the data bits into several blocks of variable number of bits, that varies depending on the modulation used. Then the blocks of bits are modulated into symbols in accordance to the constellation in use, such as QPSK, 16 QAM and 64 QAM.

Then an Inverse Fast Fourier Transform (IFFT) is applied to convert the data to convert the data in the frequency domain to the time domain. The resulting signal is then converted to serial again and a CP is added to each symbol to avoid ISI. After that, the signal is converted from digital to analogue through a Digital to Analogue Converter (DAC) and amplified by a low-noise amplifier.

On the receiver side we can see that the process shall be inverted, as after the reception and filtration of signal, it is converted again to digital through a Analog to Digital Converter

(ADC), it's CP is removed, and it's data is converted to the frequency domain through a Fast Fourier Transform (FFT). Finally, the symbols are converted yet again to serial and demodulated to obtain the expected transmitted data.

2.1.1 OFDMA

Orthogonal Frequency Division Multiple Access (OFDMA) is the multi-user version of the OFDM scheme where multiple access is achieved by assigning subsets of subcarriers to different users.

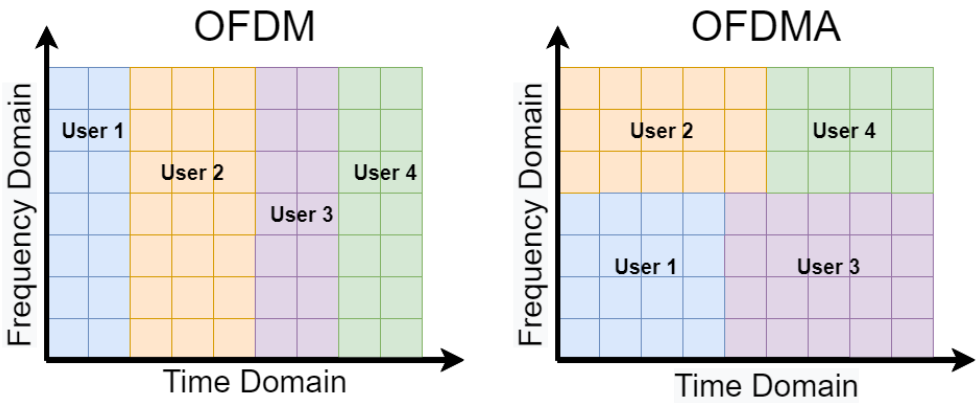

Figure 9 - Comparison of OFDM and OFDMA

As one can see in the Fig.9, OFDMA employs multiple closely spaced subcarriers like OFDM, but these are divided into dynamic blocks varying in frequency and time that can be allocated to different users. OFDMA is used in both LTE and 5G-NR technologies as it's downlink technique due to its many advantages, such as its efficient use of frequency allocation, its multi-user diversity, its simple receiver structure and, ability to cope with severe channel conditions without complex equalization filters. However, OFDMA schemes are sensitive to frequency offset, which requires its subcarriers to have appropriate frequency spacing to tolerate the Doppler shift, and they have high peak-to-average ratio (PAPR), making them inefficient in signal uplinks [28] [29].

2.2 SC-FDMA

Single Carrier FDMA (SC-FDMA) is a Frequency Division Multiple Access scheme, that combines the low PAPR of traditional single-carrier formats, such as GSM, with the multipath resistance and in-channel frequency scheduling flexibility of OFDM schemes [32]. The SC-FDMA scheme is similar to OFDMA, as it can be seen in the Fig.10, having only an additional Discrete Fourier Transform (DFT) block before the OFDM's subcarrier mapping, which is what makes this a Single-Carrier system. Unlike the standard OFDM where each data symbol is carried by the individual subcarriers, the SC-FDMA transmitter carries data symbols over a group of subcarriers transmitted simultaneously. In other words, the group of subcarriers that carry each data symbol can be viewed as one frequency band carrying data sequentially in a standard FDMA.

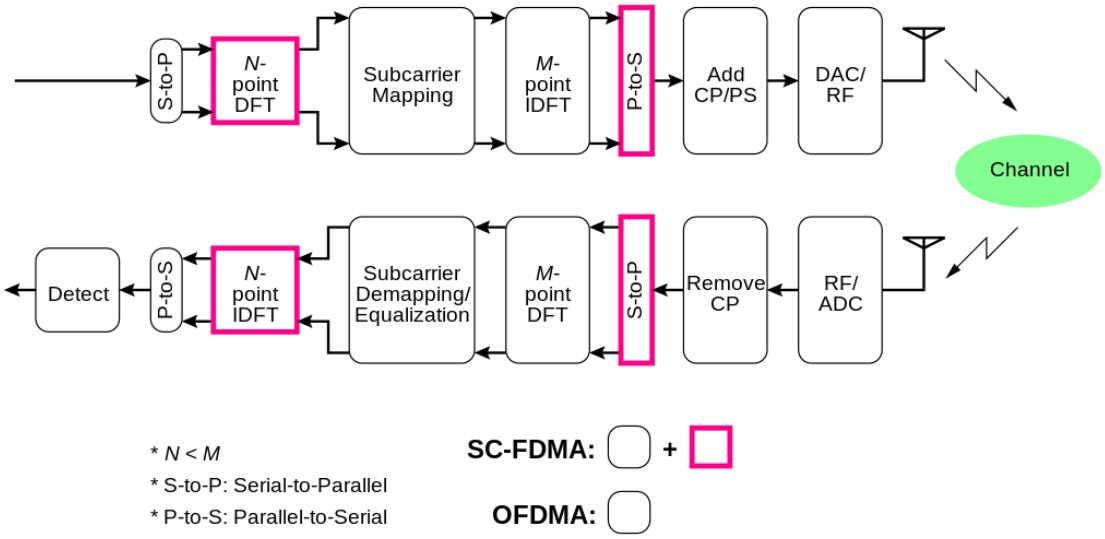

Figure 10 - Block Diagram of SC-FDMA [31]

Although the performance gap between SC-FDMA and OFDMA is relatively small, the previously mentioned SC-FDMA's advantage of low PAPR makes it suitable for wireless uplink transmission in mobile communication systems, as the power efficiency of the User Equipment (UE) terminals is extremely important due to their limited available power [34].

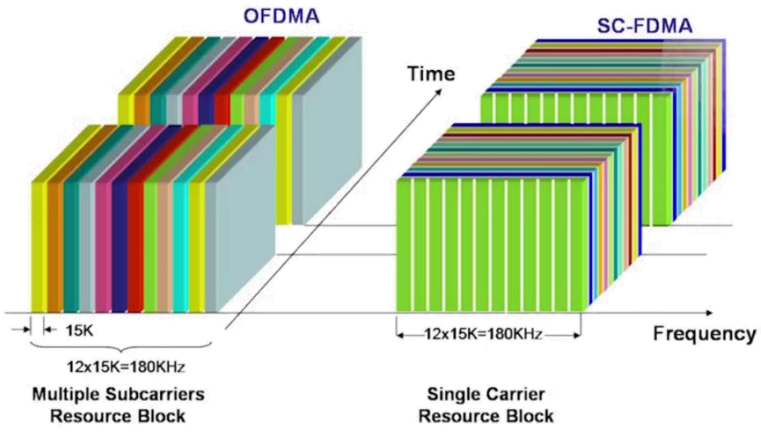

Figure 11 - Resource Block Comparison between OFDMA and SC-FDMA [35]

2.2.1 Linear Single-user Equalizers

To decide an apt equalizer for this scheme we must first analyze the SC-FDMA system in the frequency domain to verify how it can properly restore the signal's orthogonality.

Taking in account a starting signal $\mathbf{d} = [d_1, d_2, \dots, d_N]^T$, we will have the following modulated signal after the SC-FDMA DFT modulation

$$\mathbf{s} = \mathbf{Fd} \tag{2.3}$$

with **F** representing the DFT matrix of size *N* x *N*.

We then demodulate the signal with the OFDM FFT operation and send it through the $\mathbf{H_t} = \begin{bmatrix} h_1 & 0 & \dots & 0 \\ 0 & h_2 & \dots & 0 \\ \dots & \dots & \dots & \dots \\ 0 & \dots & 0 & h_N \end{bmatrix}$ channel, obtaining the received signal

$$\mathbf{y} = \mathbf{H_t F d} + \mathbf{n} \tag{2.4}$$

We then obtain the estimated signal after equalization processing

$$\mathbf{z} = \mathbf{G_t H_t F d} + \mathbf{G n} \tag{2.5}$$

With $\mathbf{G_t}$ being the equalization matrix

$$\mathbf{G_t} = \begin{bmatrix} g_1 & 0 & \dots & 0 \\ 0 & g_2 & \dots & 0 \\ \dots & \dots & \dots & \dots \\ 0 & \dots & 0 & g_N \end{bmatrix} \tag{2.6}$$

Finally, we reach the estimated detected data

$$\hat{\mathbf{d}} = \mathbf{F^{-1} G H F d} + \mathbf{F^{-1} G n} \tag{2.7}$$

With $\mathbf{F^{-1}}$ representing the IDFT matrix of size *N* x *N*

So, to ensure that the detected signal retains the original's orthogonality, the equalizer must remove the interferences added in by the channel, which results in:

$$\mathbf{GH} = \mathbf{I}_{\boldsymbol{N}} \tag{2.8}$$

Knowing this we can now quickly evaluate the performances of some of the most used single-user frequency domain equalizers when used in SC-FDMA systems [35].

- **Maximal Ratio Combining (**MRC**)**

In MRC equalizers, the receiving signals from each branch are co-phased and summed up with optimal weight. That means that the gain of each branch is made proportional to the RMS value of the signal and inversely proportional to its mean square noise level.

This equalizer coefficients can be given by:

$$g_l = h_l^*, l = 1, \dots, N \tag{2.9}$$

As it can be seen, this equalization scheme does not restore orthogonality to the detected signal and so, any variation in the channel coefficient can cause ICI.

- **Equal Gain Combining** (EGC)

EGC equalizers work very much like the MRC, with the exception that all branches are given the same weight. Its coefficients can be described as:

$$g_l = \frac{h_l^*}{|h_l^*|}, l = 1, \dots, N \tag{2.10}$$

In this case orthogonality is also not restored, and so we have present the same issues that MRC brought forth.

- **Zero Forcing Combining** (ZF)

ZFC equalizers apply the inverse of the channel frequency response to the received signal, restoring orthogonality and eliminating ICI.

$$g_l = \frac{h_l^*}{|h_l^*|^2}, l = 1, \dots, N \tag{2.11}$$

This scheme does however amplify the noise perceived at the receiver

- **Minimum Mean Square Error Combining** (MMSE)

MMSE consists on an algorithm that reduces the mean square error of the transmitted signal by taking in account the noise variance.

$$g_l = \frac{h_l^*}{|h_l^*|^2 + \sigma^2}, l = 1, \dots, N \quad (2.12)$$

Although the ICI is not totally mitigated, the trade-off in reduced noise power at the receiver results in a better performance when compared to ZF.

3. Multi-Antenna Systems

Several challenges face the progress of wireless communications as the ever-increasing demand for higher data rates and improved quality of service clashes with the limited available frequency spectrum as well as the complex nature of the wireless environment. To alleviate these issues, multi-antenna systems of special interest. By employing multiple antennas at the transmitter and/or receiver in a mobile communication system, the scattering channel can be exploited to create a multiplicity of parallel links over the same bandwidth. This usage of the spatial domain provides multi-antenna systems with several advantages, including spatial diversity gain, spatial multiplexing gain, and array gain [35].

Depending on the number of antennas used on the transmitter and receiver we can obtain four possible configurations, such as they are displayed in the Figure 4:

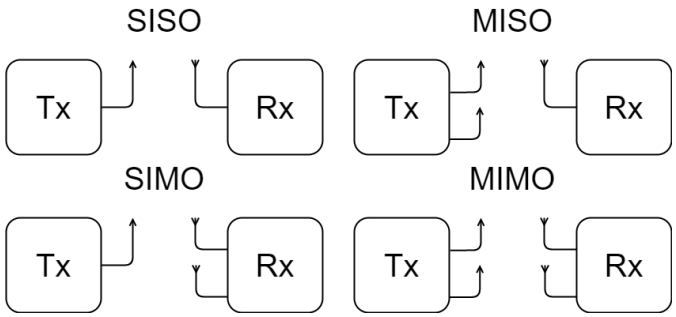

Figure 12 - Single and Multiple Antenna Schemes

As we can see, the Single Input Single Output (SISO) configuration is the simplest scheme and the one used throughout the first three generations of mobile communications.

In the Single Input Multiple Output (SIMO) configuration, the multiple antennas in the receiver enable Receive Diversity which offers better performance on non-optimal situations, such as low SNR conditions or strong fading environments thanks to its diversity and array gain.

The Multiple Input Single Output (MISO) scheme can produce Transmit Diversity through both open loop techniques, such as Space-Time Coding (STC), or through closed loop techniques, like Beamforming, to also achieve better performance on fading channel conditions.

Finally, MIMO schemes can be viewed as a mix of both SIMO and MISO configurations that can also provide a higher robustness and throughput of data capacity.

3.1 Diversity

While the above schemes provide good communication systems, their transmission channels are nonetheless subjected to reflection, diffusion, refraction, fading and co-channel interference. A natural solution to improve the performance, when faced with these issues, is to ensure that the information passes through multiple signal paths simultaneously, making sure that reliable communication is possible so long one of the paths remains strong. This technique is called diversity, and it can dramatically improve the performance over fading channels. There are many ways to obtain diversity.

Time diversity, which is achieved by sending the same information at different times, can be obtained through coding and interleaving. The information to be sent is coded and its symbols dispersed over time in different periods so that different parts of the resulting signal experience independent interference and fading. Similarly, frequency diversity can also be achieved in frequency-selective channels by transmitting the same narrowband signal at different carriers. In a channel with multiple transmit or receive antennas spaced sufficiently far apart, diversity can be obtained over space as well. Both time and frequency diversity have the drawback of providing unwanted redundancy and requiring an increased amount of scarce resources in the network throughput and bandwidth respectively. We shall now look at both the receive diversity in SIMO channels and transmit diversity in MISO channels.

3.1.1 Receive Diversity

Receive Diversity, as the name implies, consists in techniques that combine a fading signal received by multiple antennas with the objective of recovering the desired signal [36].

There are various methods to combine the received signals, such as:

- **Equal Gain Combining:** Equal weight is given to each received signal, which are then co-phased and summed.
- **Maximal Ratio Combining:** Received signals are weighted based on their SNR and are then co-phased and summed.
- **Selection Combining:** The Receiver simply chooses the strongest signal received. This method can be used with a single antenna.
- **Switched Combining:** The Receiving Antennas are scanned until a signal with above a predefined threshold is obtained, which is then used. If the signal degrades below said threshold, the Receiver scans its antennas yet again for an acceptable signal.

3.1.2 Transmit Diversity

In the Transmit Diversity case, the Transmitter that uses multiple antennas to send the same signal to reduce its fading. However, the receiver must deal with the resulting signal interference, which can be solved differently depending on feedback between receiver and transmitter of the Channel State Information (CSI). Based on the feedback requirements, transmit diversity schemes can be categorized into closed loop (CL) and open loop (OL) schemes [37].

In general, if the CSI is signaled to the transmitter then it is in a closed loop with the receiver and it can simply apply a phase shift to the signals being sent to ensure that these are received in phase of each other to avoid interference.

When the CSI is unavailable the Transmit Diversity must be established through Space-Time Coding (STC). The most used of which is the Space-Time Block Coding (STBC). These are codes created to assure orthogonal characteristics between the signals sent, obtaining then full diversity gain with simple decoding [38].

- **Space-Time Coding**

In 1998 Tarokh introduced in a space-time coding technique known as Space-Time Trellis Coding (STTC) [39]. This technique combines channel coding and transmit diversity to provide significant performance improvement. A major drawback of STTC was that the decoding complexity exponentially increased with the transmission rate.

In the same year, Alamouti presented a remarkable transmit diversity scheme using two transmit antennas [40]. Even though the scheme did not achieve as much gain as that achieved by STTC, its complexity is considerably lower since it only needs simple linear processing at the receiver. Alamouti's Scheme achieved the same diversity order as that achieved by MRC reception with one transmit and two receive antennas. The Alamouti Scheme became the foundation of a new foundation of space time codes, the aforementioned Space-Time Block Codes, that transmit data through encoded blocks distributed across both time and space.

- **Alamouti Scheme**

The Alamouti scheme is based on two information symbols, s_1 and s_2, buffered by the transmitter and transmitted in two time/frequency slots. In the first slot, the symbol s_1 is transmitted over the first antenna and simultaneously symbol s_2 is transmitted over the second antenna. In the second slot, the signal $-s^*_2$ is transmitted by the first antenna and s^*_1 is transmitted by the second antenna [35] [41].

This results in the following matrix ***S***

$$\mathbf{S} = \begin{bmatrix} s_1 & -s^*_2 \\ s_2 & s^*_1 \end{bmatrix} \tag{3.1}$$

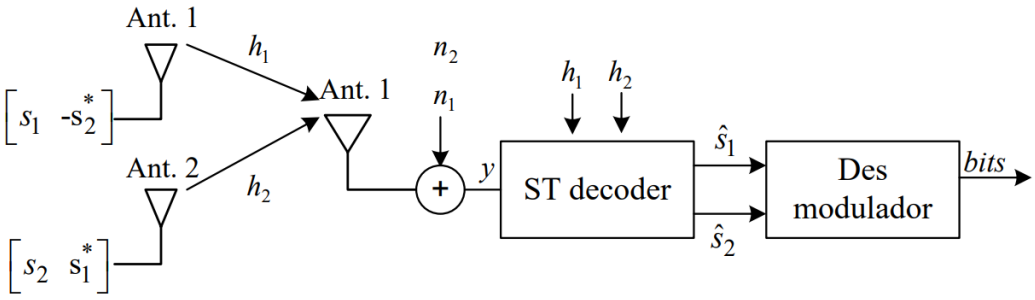

Figure 13 - Alamouti Block Diagram [35]

In a simple MISO system with two transmitting antennas, we can consider $\mathbf{h} = [h_1 \ h_2]$ as the channels between the antennas, consider $\mathbf{n} = [n_1 \ n_2]$ as the additive Gaussian noise that affects the communication between the respective time instances and $\frac{1}{\sqrt{2}}$ performing power normalization. Considering that the two time/frequency slots are highly correlated we can represent the received signal by

$$\begin{cases} y_1 = \frac{1}{\sqrt{2}} h_1 s_1 + \frac{1}{\sqrt{2}} h_2 s_2 + n_1 \\ y_2 = -\frac{1}{\sqrt{2}} h_1 s^*_2 + \frac{1}{\sqrt{2}} h_2 s^*_1 + n_2 \end{cases} \tag{3.2}$$

In the receiver it is estimated the soft decision of the data symbols $\hat{s}_1$ and $\hat{s}_2$through Alamouti decoding:

$$\begin{cases} \hat{s}_1 = \frac{1}{\sqrt{2}} h^*_1 y_1 + \frac{1}{\sqrt{2}} h_2 y^*_2 \\ \hat{s}_2 = \frac{1}{\sqrt{2}} h^*_2 y_1 \ - \frac{1}{\sqrt{2}} h_1 y^*_2 \end{cases} \tag{3.3}$$

And so, the soft decision of the data symbols results in

$$\begin{cases} \hat{s}_1 = \frac{1}{2}(h^*_1 h_1 + h_2 h^*_2) s_n + \frac{1}{\sqrt{2}} h^*_1 n_1 + \frac{1}{\sqrt{2}} h^*_1 n_2 \\ \hat{s}_2 = \frac{1}{2}(h^*_2 h_2 + h_1 h^*_1) s_n + \frac{1}{\sqrt{2}} h^*_2 n_1 - \frac{1}{\sqrt{2}} h^*_1 n_2 \end{cases} \tag{3.4}$$

Which can be further reduced into

$$\begin{cases} \hat{s}_1 = \frac{1}{2}(|h_1|^2 + |h_2|^2)s_1 + \frac{1}{\sqrt{2}}h_1^* n_1 + \frac{1}{\sqrt{2}}h_2^* n_2 \\ \hat{s}_2 = \frac{1}{2}(|h_2|^2 + |h_1|^2)s_2 + \frac{1}{\sqrt{2}}h_2^* n_1 - \frac{1}{\sqrt{2}}h_1^* n_2 \end{cases} \quad (3.5)$$

And so, having separated the symbol and noise of both antennas, we can obtain the SNR:

$$\text{SNR} = \frac{1}{2}\frac{(|h_1|^2 + |h_2|^2)}{\sigma^2} \quad (3.6)$$

From (3.5) it is possible to verify that Alamouti coding can create orthogonal codes for both antennas, as only the target symbol and Gaussian noise remains after demodulation. It should be noted that, although Alamouti coding can also be used in systems with multiple receiving antennas, it cannot maintain the signal's orthogonality in systems with more than two transmitting antennas.

3.2 Spatial Multiplexing

Under suitable channel conditions, having each antenna of a MIMO channel sending different signals provides an additional spatial dimension for communication and yields a capacity or multiplexing gain. This can be exploited by spatially multiplexing several data streams onto the MIMO channel [42], and leads to an increase in the system's capacity, as the capacity of a MIMO channel with M_T transmit and M_R receive antennas is proportional to $r=min(M_T, M_R)$.

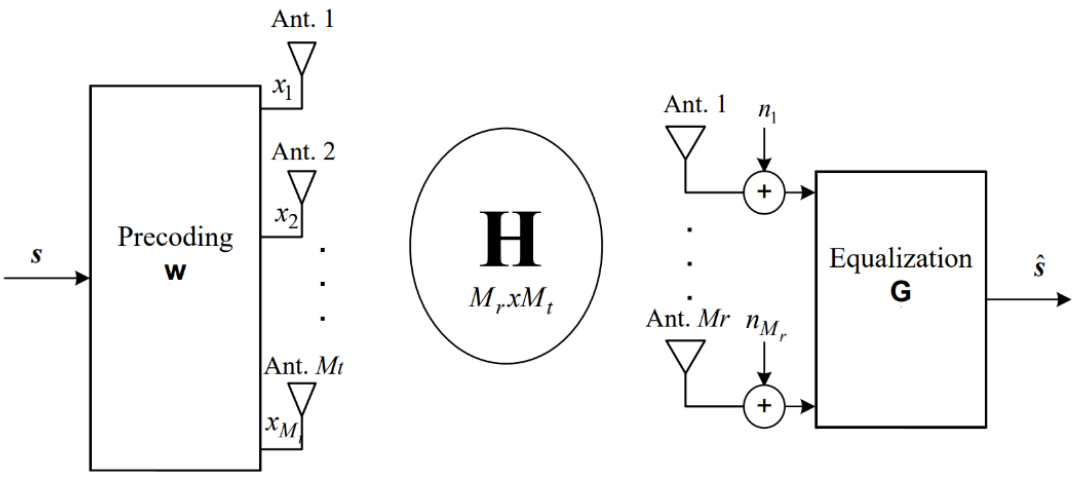

Figure 14 - Spatial Multiplexing in MIMO schemes [42]

In a MIMO channel with various transmitting and receiving antennas, the received signal $y = [y_1 \quad \cdots \quad y_{M_R}]^T$ can be represented mathematically by the equation

$$\mathbf{y} = \mathbf{Hx} + \mathbf{n} \tag{3.7}$$

Where $\mathbf{H} = \begin{bmatrix} h_{1,1} & \cdots & h_{1,M_T} \\ \vdots & \ddots & \vdots \\ h_{M_R,1} & \cdots & h_{M_R M_T} \end{bmatrix}$ is the channel matrix, $\mathbf{x} = [x_1 \quad \cdots \quad x_{M_T}]^T$ is the vector of the transmitted signal, and $\mathbf{n} = [n_1 \quad \cdots \quad n_{M_T}]^T$ the vector of the noise.

Applying the Single Value Decomposition (SVD) to the **H** matrix one can obtain

$$\mathbf{H} = \mathbf{UDV}^{\mathrm{H}} \tag{3.8}$$

Where **U** and **V** are the M_R *x r* and M_T *x r* unitary matrices and **D** a *r x r* diagonal matrix with non-negative real numbers.

$$\mathbf{D} = \begin{bmatrix} \lambda_1 & 0 & 0 \\ 0 & \ddots & 0 \\ 0 & 0 & \lambda_r \end{bmatrix} \tag{3.9}$$

The transmitted signal over the M_T antennas can be given by

$$\mathbf{x} = \mathbf{Ws} \tag{3.10}$$

Where $\mathbf{s} = [s_1 \quad \cdots \quad s_r]^T$ is the data vector and **W** the M_T *x r* precoding matrix given by:

$$\mathbf{W} = \mathbf{VP^{1/2}} \tag{3.11}$$

With **P** the *r x r* square diagonal power allocation matrix

$$\mathbf{P} = \begin{bmatrix} p_1 & 0 & 0 \\ 0 & \ddots & 0 \\ 0 & 0 & p_r \end{bmatrix}^{1/2} \tag{3.12}$$

Replacing the transmitted signal matrix **x** and the channel matrix **H** in the receiver matrix expression (3.7) with the expressions obtained in (3.8), (3.10) and (3.11), we obtain

$$\mathbf{y} = \mathbf{UDV}^{\mathrm{H}}\mathbf{VP^{1/2}s} + \mathbf{n} \tag{3.13}$$

Decodifying the transmitted signal with the matrix $\mathbf{G} = \mathbf{U}^{\mathrm{H}}$ we can obtain the estimated transmitted data symbols

$$\hat{\mathbf{s}} = \mathbf{U}^{\mathrm{H}}\mathbf{UDV}^{\mathrm{H}}\mathbf{VP^{1/2}s} + \mathbf{U}^{\mathrm{H}}\mathbf{n} \tag{3.14}$$

$$\hat{\mathbf{s}} = \mathbf{DP^{1/2}s} + \tilde{\mathbf{n}} \tag{3.15}$$

And so, the soft estimate of the *r*th data symbol is

$$\hat{s}_i = \lambda_i \sqrt{p_i} s_i + \tilde{n}_i \tag{3.16}$$

As we can see, by multiplexing an *r* number of parallel channels through the use of SVD we can transmit *r* interference free data symbols.

3.3 Multi-user Equalizers

In this section we present some multi-user equalizers common used to mitigate the interference. First, we shall start by doing an overview of linear equalizers used in SC-FDMA and then we present a nonlinear one based on IB-FDE principle [43] [44].

- **Zero-Forcing Equalizer**

ZF Equalizers apply the inverse of the channel frequency response to the received signal, restoring orthogonality and eliminating ICI. Returning to the representation of the received signal in a MIMO channel (3.7), we must now estimate the vector of the data symbols (3.17).

$$\hat{\mathbf{x}} = \mathbf{G}\mathbf{y} = \mathbf{G}\mathbf{H}\mathbf{x} + \mathbf{G}\mathbf{n} \tag{3.17}$$

It's then easy to see the solution to remove the interference, as it is the pseudo-inverted **H** matrix.

$$\mathbf{G}_{ZF} = (\mathbf{H}^H\mathbf{H})^{-1}\mathbf{H}^H \tag{3.18}$$

$$\hat{\mathbf{x}} = (\mathbf{H}^H\mathbf{H})^{-1}\mathbf{H}^H\mathbf{H}\mathbf{x} + \mathbf{G}_{ZF}\mathbf{n} = \mathbf{I}_N\mathbf{x} + \mathbf{G}_{ZF}\mathbf{n} \tag{3.19}$$

As one can verify with this equalizer, we have the issue of the noise perceived at the receiver being amplified by **G**.

- **Minimum Mean Square Error Equalizer**

MMSE equalizers minimize the Mean Square Error (MSE) between the transmitted vector *x* and it's estimate $\hat{x}$ in the receptor. The computation of the equalizer coefficient of the MMSE requires the knowledge of the noise variance σ^2 as it can be seen in the equation of the $\mathbf{G}_{MMSE}$ (3.20).

$$\mathbf{G}_{MMSE} = (\mathbf{H}^H\mathbf{H} + \sigma^2\mathbf{I}_N)^{-1}\mathbf{H}^H \tag{3.20}$$

$$\begin{aligned}\hat{\mathbf{x}} &= (\mathbf{H}^H\mathbf{H} + \sigma^2\mathbf{I}_N)^{-1}\mathbf{H}^H\mathbf{H}\mathbf{d} + \mathbf{G}_{MMSE}\mathbf{n} \\ &= \mathbf{I}_N\mathbf{x} + \mathbf{G}_{MMSE}\mathbf{n}\end{aligned} \tag{3.21}$$

Although the ICI is not totally mitigated, the trade-off in reduced noise power at the receiver results in a better performance when compared with the ZF equalizer, since only when SNR→∞ does the MMSE become identical to ZF.

3.3.1 Iterative Block Decision Feedback Equalizer

As it was shown, linear equalizers don't fully mitigate residual ICI, which brings concerning issues in mobile networks as the channel time-variation caused by Doppler shift in moving UEs is both inevitable and the main cause of ICI [45].

A better and more robust solution to the interference issue arrives with iterative space-frequency equalizations, namely IB-DFE, which has been proposed to deal with ICI and efficiently separate the spatial streams without requiring perfect CSI knowledge by the transmitters. We shall now briefly describe the concept of IB-DFE as it will be used to design the proposed scheme in the next chapter [46].

To simplify the discussion let's assume a single user and single antenna scenario, i.e. it is assumed a single antenna transmitter and a single antenna receiver, as it can be seen in the Fig.15. This equalizer architecture includes two filters: The first, a feedforward filter, equalizes most of the interference while the second one, the feedback filter, attempts to remove the ICI and some of the residual interference. As this is an iterative process, it gradually increases the reliability of the received data.

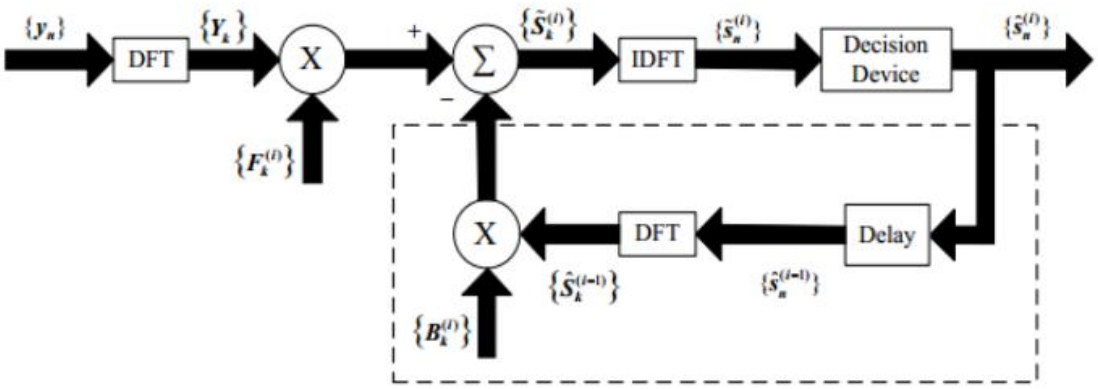

Figure 15 - Basic IB-DFE block diagram [47]

At the *i*-th iteration, the operation of the output of this frequency-domain block is:

$$\tilde{S}_k^{(i)} = F_k^{(i)} Y_k - B_k^{(i)} \hat{S}_k^{(i-1)} \tag{3.22}$$

Where $F_k^{(i)}$ is the feedforward coefficient and $B_k^{(i)}$ the feedback coefficient from the IB-DFE block.

The feedforward and feedback coefficients are chosen in order to maximize the Signal-to-Interference-Noise Ratio (SINR) and given by:

$$F_k^{(i)} = \frac{H_k^H}{\sigma^2 + (1 - (\rho^{(i-1)})^2)|H_k|^2} \tag{3.23}$$

And

$$B_k^{(i)} = \rho^{(i-1)}(F_k^{(i)} H_k - 1) \tag{3.24}$$

With ρ representing the correlation coefficient that ensures a good performance at the receiver as it supplies a reliability measure of the estimates employed at the feedback loop.

4. Design and implementation of a robust IB-DFE for SC-FDMA Systems

It is well known that linear multi-user equalizers are not the best ones for SC-FDMA systems due to the residual interference. It has been shown that nonlinear/iterative multi-user equalizers, in particular the ones based on the IB-DFE principle, outperforms linear ones and have excellent performance-complexity tradeoffs [48]. However, most of the nonlinear equalizers such as IB-DFE were designed by assuming perfect CSI and since in practical systems the channel faces errors the performance may be far from the ideal. Therefore, in this Chapter a robust IB-DFE is derived and evaluated. In the design we assume errors in the channels. The equalizer matrices are computed by minimizing the mean square error (MSE) of all users at each subcarrier by explicitly assuming that the channels have errors. It is considered a set of single antenna user terminals transmitting, using the same radio resources, to a multi-antenna base station. The designed scheme allows an efficient user separation even under imperfect CSI, with a performance close to the one given by the matched filter bound with only a few iterations.

4.1 System model

As previously stated, the Fig.16 shows the considered uplink SC-FDMA-based transmitter of the *k*-th user. We shall consider a base station equipped with *M* antennas and *K* single antenna UEs whose information is transmitted at the same frequency band.

A SC-FDMA scheme is employed by each UE with the data blocks associated to the *k*-th UE (k=1,…K) being $\{s_{k,n}; n = 0, \dots, L-1\}$, where the constellation symbol $S_{k,n}$ is selected from the data according to the chosen mapping rule. The L-length data block symbols are moved to the frequency domain obtaining $\{S_{k,l}; l = 0, \dots, L-1\} = \text{DFT}\{s_{k,l}; l = 0, \dots, L-1\}$. The frequency domain signals are then interleaved so that they are widely separated in the OFDM symbol, therefore increasing the frequency diversity order. Finally, the OFDM modulation is performed and a cyclic prefix inserted.

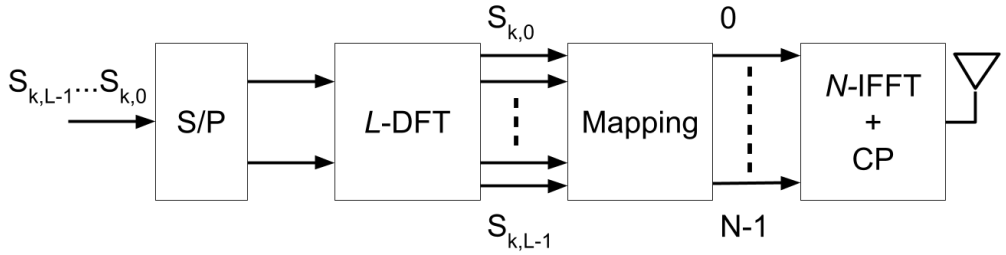

Figure 16 - SC-FDMA based transmitter [46]

The received signal on the *l* subcarrier can then be expressed as:

$$\mathbf{Y}_l = \mathbf{H}_l^T \mathbf{S}_l + \mathbf{N}_l \tag{4.1}$$

With $\mathbf{Y}_l = \left[Y_l^{(1)} \dots Y_l^{(M)}\right]^T$, $\mathbf{N}_l = \left[N_l^{(1)} \dots N_l^{(M)}\right]^T$, $\mathbf{S}_l = \left[S_{1,l} \dots S_{k,l}\right]^T$, and $\mathbf{H}_l^T = \begin{bmatrix} H_{1,l}^{(1)} & \cdots & H_{k,l}^{(1)} \\ \vdots & \ddots & \vdots \\ H_{1,l}^{(\mathrm{M})} & \cdots & H_{k,l}^{(\mathrm{M})} \end{bmatrix}$.

4.2 Multi-user IB-DFE under perfect CSI

In Sec. 3.4 we looked into the basics of IB-DFE for single carrier systems when considering only one user. We shall now approach the equalizer through a multi-user scheme which obtains the equalizer matrices by minimizing the overall MSE of the receiving signals at each subcarrier as can be seen in Fig.17 [46].

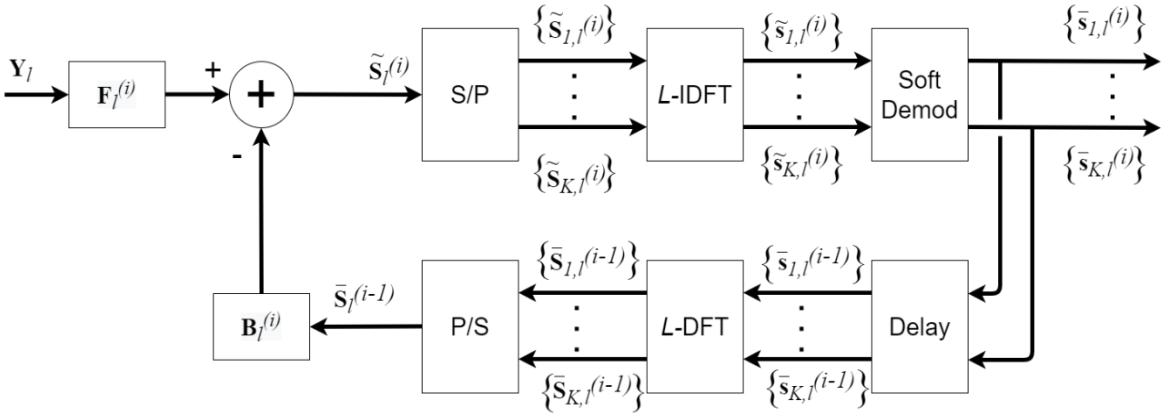

Figure 17 - Block Diagram of the IB-DFE PIC Receiver

From Fig. 16 and 17, the received signal on the *l*-th subcarrier of all UEs, before the *L*-IDFT operation, is given by

$$\tilde{\mathbf{S}}_l^{(i)} = \mathbf{F}_l^{(i)T}\mathbf{Y}_l - \mathbf{B}_l^{(i)T}\bar{\mathbf{S}}_l^{(i-1)} \tag{4.2}$$

Where $\mathbf{F}_l^{(i)} = \left[\mathbf{F}_{1,l}^{(i)} \dots \mathbf{F}_{K,l}^{(i)}\right]$ is a matrix of size *M* x *K* with all UEs' feedforward vector coefficients, $\mathbf{B}_l^{(i)} = \left[\mathbf{B}_{1,l}^{(i)} \dots \mathbf{B}_{K,l}^{(i)}\right]^T$ is a matrix of size *K* x *K* with all UEs' feedback vector coefficients, $\tilde{\mathbf{S}}_l^{(i)} = \left[\tilde{\mathbf{S}}_{1,l}^{(i)} \dots \tilde{\mathbf{S}}_{K,l}^{(i)}\right]^T$, and $\bar{\mathbf{S}}_l^{(i-1)}$ is the soft decisions' vector of the previous iteration that can be assumed to be

$$\bar{\mathbf{S}}_l^{(i-1)} \approx \mathbf{P}^{(i-1)} \ \mathbf{S_l} + \mathbf{\Delta_l}^{(i-1)} \tag{4.7}$$

with the mean error vector $\mathbf{\Delta_l} = [\Delta_{1,l} \ \dots \ \Delta_{K,l}]^T$ and the matrix of correlation coefficients defined as $\mathbf{P} = \begin{bmatrix} \rho_1 & 0 & 0 \\ 0 & \ddots & 0 \\ 0 & 0 & \rho_k \end{bmatrix}$. The correlation coefficient represents the reliability of the estimates used in the feedback loop to the *k*-th user, and can be given by [49],

$$\rho_k = \frac{\mathbb{E}\left[\hat{s}_{k,n}s_{k,n}^*\right]}{\mathbb{E}\left[\left|s_{k,n}\right|^2\right]} = \frac{\mathbb{E}\left[\hat{S}_{k,l}S_{k,l}^*\right]}{\mathbb{E}\left[\left|S_{k,l}\right|^2\right]} \tag{4.8}$$

As we are using a QPSK constellation we have

$$s_{k,n} = s_{k,n}^I + js_{k,n}^Q = \ \pm d \ \pm jd \tag{4.8}$$

Where $s_n^I = \mathrm{Re}\{s_{k,n}\}$ and $s_n^Q = \ \mathrm{Im}\{s_{k,n}\}$ are the in-phase" and quadrature components of s_n while *d=D/2*, with *D* being the minimum Euclidean distance, so considering a normalized QPSK constellation we have $s_{k,n} = \ \pm 1 \ \pm j1$. Which means that the symbol estimate can be written as

$$\bar{s}_{k,n} = \tanh\left(\frac{L_{k,n}^I}{2}\right) + j\tanh\left(\frac{L_{k,n}^Q}{2}\right) \tag{4.3}$$

With the Log Likelihood Ratios (LLRs) of the in-phase component (L_n^I) and the quadrature component (L_n^Q) given by

$$\begin{cases} L_{k,n}^{I} = \dfrac{2}{\sigma_{k,n}^{2}} \mathrm{Re}\{\tilde{s}_{k,n}\} \\ L_{k,n}^{Q} = \dfrac{2}{\sigma_{k,n}^{2}} \mathrm{Im}\{\tilde{s}_{k,n}\} \end{cases} \tag{4.4}$$

where

$$\sigma_{k,n}^{2} = \frac{1}{2}\mathbb{E}\left[\left|s_{k,n'} - \bar{s}_{k,n'}\right|\right] = \frac{1}{2L}\sum_{n'=0}^{L-1}\left|\hat{s}_{k,n'} - \bar{s}_{k,n'}\right|^{2} \tag{4.5}$$

The hard decisions $\hat{s}_{k,n}^{I} = \pm 1$ and $\hat{s}_{k,n}^{Q} = \pm 1$ are defined according to signs of $L_{k,n}^{I}$ and $L_{k,n}^{Q}$, while the in-phase and quadrature components of the correlation coefficient of the *k*-th user is given by

$$\begin{cases} \rho_{k,n}^{\mathrm{I}} = \dfrac{\mathbb{E}\left[\hat{s}_{k,n}^{I} s_{k,n}^{I}\right]}{\mathbb{E}\left[\left|s_{k,n}^{I}\right|^{2}\right]} = \tanh\left(\dfrac{\left|L_{k,n}^{\mathrm{I}}\right|}{2}\right) \\ \rho_{k,n}^{\mathrm{Q}} = \dfrac{\mathbb{E}\left[\hat{s}_{k,n}^{Q} s_{k,n}^{Q}\right]}{\mathbb{E}\left[\left|s_{k,n}^{Q}\right|^{2}\right]} = \tanh\left(\dfrac{\left|L_{k,n}^{\mathrm{Q}}\right|}{2}\right) \end{cases} \tag{4.9}$$

And so, the correlation coefficient can be approximated to

$$\rho_{k} \approx \frac{1}{2L}\sum_{n=0}^{L-1}(\rho_{k,n}^{\mathrm{I}} + \rho_{k,n}^{\mathrm{Q}}) \tag{4.8}$$

For a given iteration and the detection of the *k*-th UE, the iterative receiver equalizer is composed by the coefficients $\mathbf{F}_{l}^{(i)}$ and $\mathbf{B}_{l}^{(i)}$ which are computed to minimize the average BER of all UEs and for a QPSK constellation with Gray mapping, the average BER can be approximately given by

$$\mathrm{BER} \approx Q\left(\sqrt{\frac{K}{\frac{1}{L}\sum_{l=0}^{L-1}\mathrm{MSE}_{l}}}\right) \tag{4.10}$$

Where $Q(.)$ denotes the Q-function and MSE_{l} the overall mean square error on the frequency domain samples, which is given by

$$\mathrm{MSE}_{l} = \mathbb{E}\left[\left\|\tilde{\mathbf{S}}_{l}^{(i)} - \mathbf{S}_{l}\right\|^{2}\right] = \left[tr\left(\left(\tilde{\mathbf{S}}_{l}^{(i)} - \mathbf{S}_{l}\right)\left(\tilde{\mathbf{S}}_{l}^{(i)} - \mathbf{S}_{l}\right)^{H}\right)\right] \tag{4.11}$$

After some mathematical manipulation, it can be shown that

$$\begin{aligned}\mathrm{MSE}_l = \mathrm{tr}\left(\mathbf{F}_l^H \mathbf{R}_l^{\mathbf{Y}} \mathbf{F}_l\right) + \mathrm{tr}\left(\mathbf{B}_l^H \mathbf{R}^{\bar{\mathbf{S}},\bar{\mathbf{S}}} \mathbf{B}_l\right) + K\sigma_s^2 - 2\mathrm{tr}\left(\mathrm{Re}\left\{\mathbf{F}_l^H \mathbf{R}_l^{\mathbf{Y},\mathbf{S}}\right\}\right) \\ + 2\mathrm{tr}\left(\mathrm{Re}\left\{\mathbf{B}_l^H \mathbf{R}^{\bar{\mathbf{S}},\mathbf{S}}\right\}\right) - 2\mathrm{tr}\left(\mathrm{Re}\left\{\mathbf{B}_l^H \mathbf{R}_l^{\bar{\mathbf{S}},\mathbf{Y}} \mathbf{F}_l\right\}\right)\end{aligned} \tag{4.12}$$

With

$$\begin{cases} \mathbf{R}_l^{\mathbf{Y}} = \mathbb{E}[\mathbf{Y}_l^* \mathbf{Y}_l^T] = \mathbf{H}_l^H \boldsymbol{\sigma}_S^2 \mathbf{I}_K \mathbf{H}_l + \boldsymbol{\sigma}_N^2 \mathbf{I}_N \\ \mathbf{R}^{\bar{\mathbf{S}},\bar{\mathbf{S}}} = \mathbb{E}[\bar{\mathbf{S}}^* \bar{\mathbf{S}}^T] = \mathbf{P}^2 \boldsymbol{\sigma}_S^2 \mathbf{I}_K \\ \mathbf{R}_l^{\mathbf{Y},\mathbf{S}} = \mathbb{E}[\mathbf{Y}_l^* \mathbf{S}_l] = \mathbf{H}_l^H \boldsymbol{\sigma}_S^2 \mathbf{I}_K \\ \mathbf{R}^{\bar{\mathbf{S}},\mathbf{S}} = \mathbb{E}[\bar{\mathbf{S}}^* \mathbf{S}_l] = \mathbf{H}_l^H \boldsymbol{\sigma}_S^2 \mathbf{I}_K \\ \mathbf{R}_l^{\bar{\mathbf{S}},\mathbf{Y}} = \mathbb{E}[\bar{\mathbf{S}}^* \mathbf{Y}_l] = \mathbf{P}^2 \boldsymbol{\sigma}_S^2 \mathbf{I}_K \mathbf{H}_l \end{cases} \tag{4.13}$$

From (4.12), we can see that to minimize the BER we need to minimize the overall MSE at each subcarrier. This may lead to biased estimates, so to avoid this issue we force the received amplitude to *K*

$$\min_{\mathbf{F}_l \mathbf{B}_l} MSE_l \; s.t \; \frac{1}{L} \sum_{l=0}^{L-1} \mathbf{F}_l^T \mathbf{H}_l^T = K \tag{4.14}$$

By applying the Karush-Kuhn-Tucker (KKT) condition to solve the optimization problem we obtain the solution [49] [50]:

$$\mathbf{F}_l^{(i)} = \left(\mathbf{H}_l^H \left(\mathbf{I}_K - \mathbf{P}^{(i-1)^2} \right) \mathbf{H}_l + \frac{\sigma_N^2}{\sigma_S^2} \mathbf{I}_l \right)^{-1} \mathbf{H}_l^H \boldsymbol{\Omega}^{(i)} \tag{4.15}$$

And

$$\mathbf{B}_l^{(i)} = \mathbf{H}_l \mathbf{F}_l^{(i)} - \mathbf{I}_k \tag{4.16}$$

With

$$\boldsymbol{\Omega}^{(i)} = \left(\mathbf{I}_K - \mathbf{P}^{(i-1)^2} \right) - \frac{\mu^{(i)}}{\sigma_s^2 L} \mathbf{I}_k \tag{4.17}$$

After which, the Lagrangian multiplier is selected, at each iteration *i*, to ensure the constraint $\frac{1}{L} \sum_{l=0}^{L-1} tr(\mathbf{F}_l^T \mathbf{H}_l^T) = K$.

Since all users are detected in parallel, for the first iteration (i=1), the IB-DFE reduces to the conventional multi-user MMSE in the frequency domain, since $\mathbf{P}^{(o)}$ is a null matrix and $\bar{\boldsymbol{S}}_l^{(0)}$ is a null vector.

4.3 Robust IB-DFE under imperfect CSI

In this section we design a robust IB-DFE by explicitly assuming imperfect CSI. The criterion to derive the equalizer matrices is the same as the perfect case, i.e., minimization of the MSE of all users at each subcarrier.

In practical systems the channel must be estimated at the receiver side, but this estimation is always done with errors. This can be mathematically simulated by,

$$\mathbf{H'}_l = \mathbf{H}_l + \mathbf{E}_l \tag{4.18}$$

Where $\boldsymbol{H'}_l$ represents the estimated channel, $\mathbf{H}_l$ the perfect channel and $\mathbf{E}_l$ the channel error estimation, modeled as,

$$\mathbb{E}[\mathbf{E}_l \mathbf{E}_l^H] = \sigma_E^2 \boldsymbol{I}_l \tag{4.19}$$

With $\mathbb{E}[.]$, in this case, representing the variance of the added error. From eq (4.18) the perfect channel can be written as,

$$\mathbf{H}_l = \mathbf{H}'_l - \mathbf{E}_l \tag{4.20}$$

From which obtain the new received signal:

$$\mathbf{Y}'_l = (\mathbf{H'}_l^T - \mathbf{E}_l)\mathbf{S}_l + \mathbf{N}_{\boldsymbol{l}} \tag{4.21}$$

We now repeat the IB-DFE process, as was shown previously, with the new estimation error added. Starting by applying the new received signal (4.21) and (4.7) unto (4.2) to obtain the new processed signal before the *L*-IDFT operation

$$\tilde{\mathbf{S}}_l^{(i)} = \mathbf{F}_l^{(i)T}\mathbf{H'}_l^T\mathbf{S}_l - \mathbf{F}_l^{(i)T}\mathbf{E}_l\mathbf{S}_l + \mathbf{F}_l^{(i)T}\mathbf{N}_{\boldsymbol{l}} - \mathbf{B}_l^{(i)T}\mathbf{P}^{(i-1)}\mathbf{S}_l - \mathbf{B}_l^{(i)T}\boldsymbol{\Delta}_{\boldsymbol{l}}{}^{(i-1)} \tag{4.22}$$

With the error being given by

$$\begin{aligned} \boldsymbol{\Delta}_{\boldsymbol{l}}{}^{(i)} &= \tilde{\mathbf{S}}_l^{(i)} - \mathbf{S}_l \\ &= \left(\mathbf{F}_l^{(i)T}\mathbf{H'}_l^T - \mathbf{F}_l^{(i)T}\mathbf{E}_l - \mathbf{B}_l^{(i)T}\mathbf{P}^{(i-1)} - \mathbf{I}_K\right)\mathbf{S}_l + \mathbf{F}_l^{(i)T}\mathbf{N}_{\boldsymbol{l}} - \mathbf{B}_l^{(i)T}\boldsymbol{\Delta}_{\boldsymbol{l}}{}^{(i-1)} \end{aligned} \tag{4.23}$$

Taking in account both (4.11) and (4.19) we can prove that $\mathrm{MSE}_l = \mathbb{E}\left[\left\|\boldsymbol{\Delta}_{\boldsymbol{l}}{}^{(i)}\right\|^2\right]$, which, when also considering

$$\begin{cases} \mathbb{E}[\mathbf{E}_l \mathbf{E}_l^H] = \sigma_E^2 \mathbf{I}_L \\ \mathbb{E}[\boldsymbol{\Delta}_l \boldsymbol{\Delta}_l^H] = \sigma_s^2(\mathbf{I}_K - \mathbf{P}^2) \\ \mathbb{E}[\mathbf{S}_l \mathbf{S}_l^H] = \sigma_s^2 \mathbf{I}_K \\ \mathbb{E}[\mathbf{N}_l \mathbf{N}_l^H] = \sigma_N^2 \mathbf{I}_L \end{cases} \tag{4.24}$$

Allows us to obtain the following MSE_l expression

$$\begin{aligned}\mathrm{MSE}_l = &\left\|\mathbf{F}_l^{(i)T}\mathbf{H}'^{T}_l - \mathbf{B}_l^{(i)T}\mathbf{P}^{(i-1)} - \mathbf{I}_K\right\|^2\sigma_s^2 \\ &+ \left\|\mathbf{B}_l^{(i)T}\left(\mathbf{I}_K - \left|\mathbf{P}^{(i-1)}\right|^2\right)^{1/2}\right\|^2\sigma_s^2 \\ &+ \left\|\mathbf{F}_l^{(i)T}\right\|(\sigma_N^2 + \sigma_E^2\sigma_s^2)\end{aligned} \tag{4.25}$$

And by once again applying the KKT condition we can obtain the new feedforward and feedback matrices

$$\mathbf{F}_l^{(i)} = \left(\mathbf{H}_l^H\left(\mathbf{I}_L - \mathbf{P}^{(i-1)^2}\right)\mathbf{H}_l + \left(\frac{\sigma_N^2}{\sigma_S^2} + \sigma_E^2\right)\mathbf{I}_L\right)^{-1}\mathbf{H}_l^H\mathbf{\Omega}^{(i)} \tag{4.26}$$

And

$$\mathbf{B}_l^{(i)} = \mathbf{H}_l\mathbf{F}_l^{(i)} - \mathbf{I}_K \tag{4.27}$$

With

$$\mathbf{\Omega}^{(i)} = \left(\mathbf{I}_K - \mathbf{P}^{(i-1)^2}\right) - \frac{\mu^{(i)}}{\sigma_s^2 L}\mathbf{I}_k \tag{4.28}$$

4.4 Performance Results

We shall now compare a set of performance results between the proposed robust system, with SC-FDMA-based transmitters and a robust IB-DFE-based receiver, with the equivalent conventional IB-DFE-based receiver, for the perfect and imperfect CSI situations:

1. Two single-antenna Transmitters (K=2) and a Receiver equipped with two antennas (M=2)
2. Four single-antenna Transmitters (K=4) and a Receiver equipped with four antennas (M=4)

In both scenarios, the main parameters used in the simulation are

Variable	**Value**
FFT size	128
Useful Subcarriers	1024
Guard Interval Subcarriers	80
Sampling Frequency	15.26 MHz
Useful symbol duration	66.6 μs
Cyclic prefix duration	5.21 μs
Overall OFDM symbol duration	71.86 μs
Subcarrier separation	15 kHz
Frame size	10 OFDM symbols
Modulation	QPSK

Table 2 - System Parameters

The channel between each transmitter and the receiver is uncorrelated and severely time dispersive, each one with rich multipath propagation, uncorrelated Rayleigh fading for different multipath components and perfect synchronization. Especially, we assume a $L_p = 32$-path frequency-selective block Rayleigh fading channel with uniform power delay profile (i.e., each path with average power of $1/L_p$). The same conclusions could be drawn for other multipath fading channels, provided that the number of separable multipath components is high. The results are presented in terms of the average BER as a function of normalized carrier-to-noise ratio, which is given by the bit energy (E_b) average bit to the noise power spectral density (N_o) and is expressed in dB.

To these results it is applied the following channel estimation error variance

$$\sigma_E^2 = 10^{-\frac{Eb/N0}{10}} \tag{4.28}$$

4.4.1 Scenario 1 – MIMO 2x2

In the Fig. 18 we compare the performance between the IB-DFE receiver with perfect and imperfect CSI with the performance of the robust IB-DFE as proposed in Sec. 4.2.2. In Fig. 19 we analyze the robustness of the proposed scheme by considering multiple channel estimation error variances.

Starting with Fig. 18 we can immediately see that, as expected, the conventional IB-DFE receiver suffers a penalty of more than 4 dB for BER = 10^{-2} in its fourth iteration, with no further improvements being found in subsequent iterations. With the use of the robust equalizer, that takes into account the channel estimation error, we can significantly decrease this penalty to less than 1dB in just four iterations.

Analyzing now the Fig. 19 we can verify that, with different values for the variance of the channel estimation error the performance curves all come close to the ideal value, with negligible differences for BER = 10^{-4}, thus proving the robustness of the modified IB-DFE scheme.

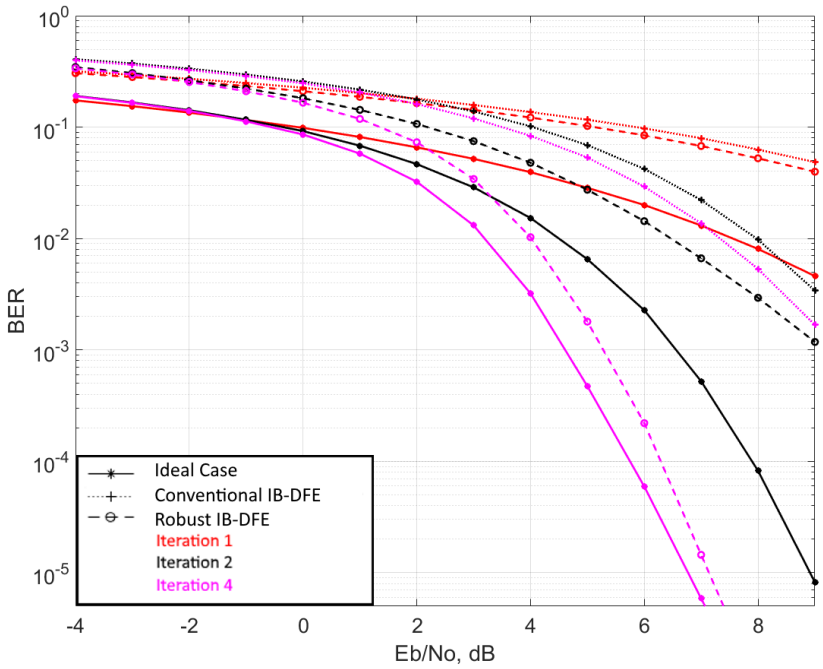

Figure 18 - Performance comparison of the IB-DFE in an ideal case with Perfect CSI with the conventional IB-DFE and robust IB-DFE with Imperfect CSI - MIMO [2x2]

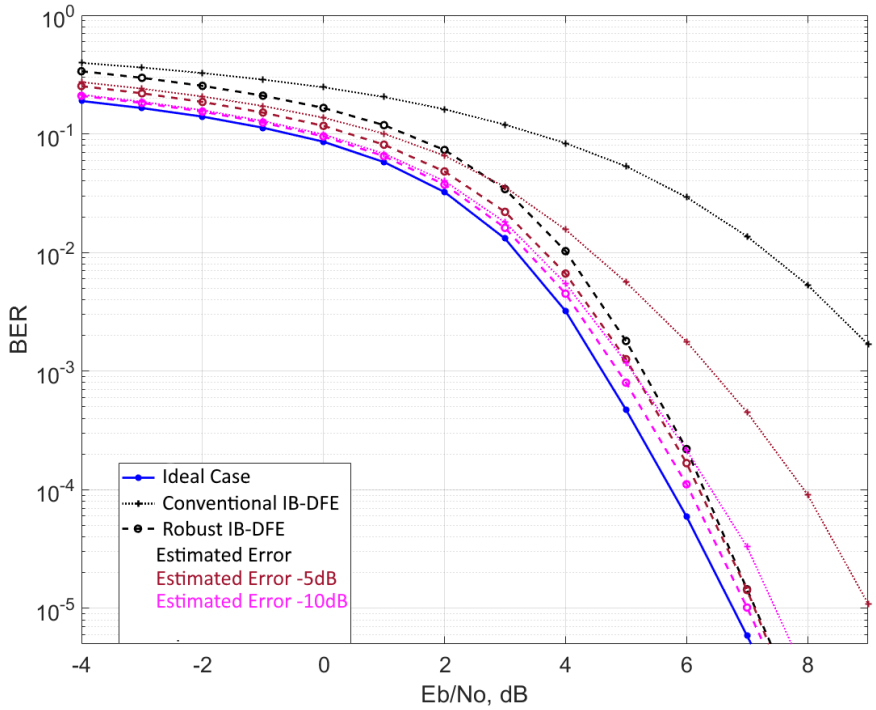

Figure 19 - Comparison of IB-DFE Performance based on the Channel Estimation Error Variance - MIMO [2x2]

4.4.2 Scenario 2 – MIMO 4x4

Considering a scenario with four single-antenna transmitters and four-antenna MIMO receiver, we can see inspecting Fig. 20 that the additional antennas have improved the systems performance. Additionally, we can also see a penalty of approximately 2dB for BER = 10^{-4} for the robust system's performance when compared to the ideal case.

The Fig. 21 shows that, in this case that we have additional antennas we have decreased the robustness of the system, as the curves for the robust IB-DFE remain apart by 1dB to 5dB from the ideal case for BER = 10^{-4}.

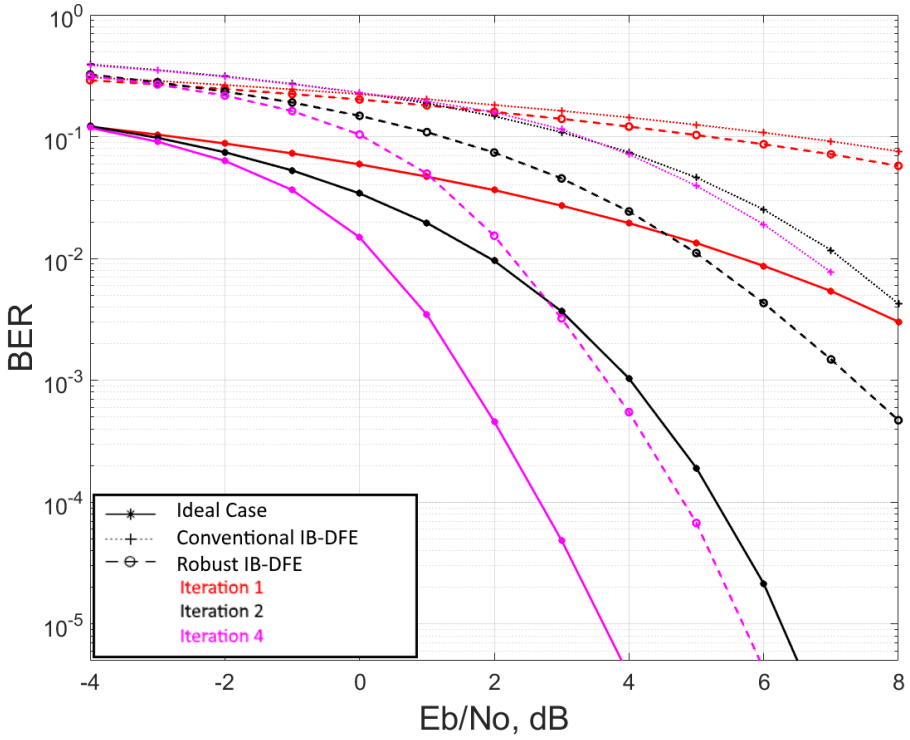

Figure 20 - Performance comparison of the IB-DFE in an ideal case with Perfect CSI with the conventional IB-DFE and robust IB-DFE with Imperfect CSI - MIMO [4x4]

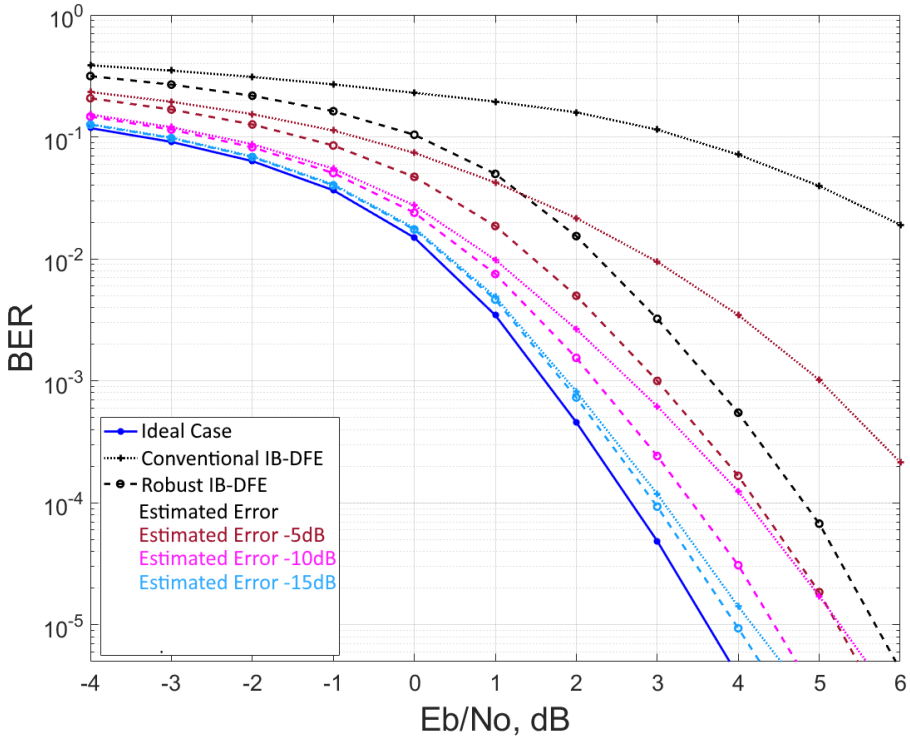

Figure 21 - Comparison of IB-DFE Performance based on the Channel Estimation Error Variance - MIMO [4x4]

5. Conclusion

In this new generation of mobile communication systems, there is a need for sophisticated interference mitigation techniques to meet the ever-increasing demand for improved throughput despite the limited frequency/time resources. Iterative equalization and other such iterative processing techniques have become increasingly popular in reducing interference. These, however, require exact knowledge of CSI which is in practice unrealistic. So, the main objective of this dissertation was the development and study of a proposed robust iterative equalization scheme, able to withstand imperfect estimates of the CSI.

In this dissertation we started with a quick overview of the evolution of mobile communications and a brief discussion of the important technologies surrounding the newly established 5G.

In the following chapter it was introduced modulation schemes used in network communication, that being OFDM, OFDMA, SC-FDE, and SC-FDMA. Chapter three presented downlink and uplink schemes used on multi-antennas systems that allow for diversity and multiplexing, as well as possible equalization techniques.

In chapter four, it was presented a system that studies the performance of multi-user IB-DFE-based receivers when the channel state information is imperfect through a flexible and developed simulation platform that allows for the configuration of the number of antennas in the receiver and transmitter, error variance, modulation, number of sub-carriers, and other such parameters.

Through the analysis of the simulation results it's possible to conclude that the proposed IB-DFE scheme, when compared to the conventional IB-DFE scheme, is able to overcome the degradation imposed by the channel estimation error in only four iterations, reaching performance values comparatively close to the ideal case. By studying the system performance for various variances of the channel estimation error we can perceive it to be generally robust to these channel estimation errors as the robust IB-DFE converges to the ideal case, proving its robustness and making it a suitable option for practical usage in mobile networks. It is also possible to see that by increasing the number of antennas in the system, the signal performance is improved.

5.1 Future Work

The focus of this dissertation was the development of a robust iterative equalization technique capable of handling imperfect channel state information. This could be further developed by considering the following:

- It would be interesting to perceive the effects of imperfect timing synchronization and pilot contamination on the performance of the proposed systems.
- In the studied systems, only single-antenna systems were used for Transmitters. Further study could involve using multiple-antenna Transmitters.
- The studied system only took in consideration the signals with subcarrier duration of 15kHz. Further study could consider the four remaining subcarrier durations used in 5G NR.

6. Bibliography

[1] Scourias, John, (1995) “Overview of the Global System for Mobile Communications, University of Waterloo.

[2] Dethan, Jacob. (2015). Wireless Broadband (UMTS). 10.13140/RG.2.1.1842.3766.

[3] Astely, David & Dahlman, Erik & Furuskar, Anders & Y, Y. & Stattin, Magnus & Parkvall, Stefan. (2009). LTE: The Evolution of Mobile Broadband. Communications Magazine, IEEE. 47. 44 - 51. 10.1109/MCOM.2009.4907406.

[4] Maskooki, Arash & Sabatino, Gabriele & Mitton, Nathalie. “Modeling and Simulation of Computer Networks and Systems”. 2015. Pages 601-627.

[5] Ahmadi, Sassan. “5G NR”, “Chapter 1 - 5G Network Architecture”,Academic Press, 2019.

[6] Sahlli, Ehab & Ismail, Mahamod & Nordin, Rosdiadee & Abdulah, Nor. (2017). Beamforming techniques for massive MIMO systems in 5G: overview, classification, and trends for future research. Frontiers of Information Technology & Electronic Engineering. 18. 753-772. 10.1631/FITEE.1601817.

[7] A. A. Zaidi, R. Baldemair, V. Moles-Cases, N. He, K. Werner and A. Cedergren, "OFDM Numerology Design for 5G New Radio to Support IoT, eMBB, and MBSFN," in *IEEE Communications Standards Magazine*, vol. 2, no. 2, pp. 78-83, JUNE 2018, doi: 10.1109/MCOMSTD.2018.1700021.

[8] Microwaves & RF, website, Jan. 2021 https://www.mwrf.com/technologies/systems/article/21849083/what-role-will-millimeter-waves-play-in-5g-wireless-systems

[9] EverythingRF, “What is Beamforming., Jan. 2021 https://www.everythingrf.com/community/what-is-beamforming

[10] “T-Mobile CZ, Huawei trial Massive MIMO in Prague”. website. Jan. 2021. https://halberdbastion.com/intelligence/news/t-mobile-cz-huawei-trial-massive-mimo-prague

[11] C. Bouras, A. Kollia and A. Papazois, "SDN & NFV in 5G: Advancements and challenges," *2017 20th Conference on Innovations in Clouds, Internet and Networks (ICIN)*, Paris, 2017, pp. 107-111, doi: 10.1109/ICIN.2017.7899398.

[12] Ying Zhang, "SDN and NFV in 5G," in *Network Function Virtualization: Concepts and Applicability in 5G Networks* , IEEE, 2018, pp.109-146, doi: 10.1002/9781119390633.ch5.

[13] 5G Subscription Forecast, website, Jan. 2021 https://www.5gamericas.org/resources/charts-statistics/

[14] Cisco Annual Internet Report, 2018–2023

[15] J. Zander, "Beyond the Ultra-Dense Barrier: Paradigm Shifts on the Road Beyond 1000x Wireless Capacity", IEEE Wireless Commun., vol. 24, no. 3, pp. 96-102, 2017.

[16] 5G Subscription Forecast, website, Dec. 2020 https://www.5gamericas.org/resources/charts-statistics/

[17] Terre, M. & Pischella, Mylène & Vivier, Emmanuelle. (2013). OFDM and LTE. 10.1002/9781118625422.ch4.

[18] U. Kumar, C. Ibars, A. Bhorkar and H. Jung, "A Waveform for 5G: Guard Interval DFT-s-OFDM," *2015 IEEE Globecom Workshops (GC Wkshps)*, San Diego, CA, 2015, pp. 1-6, doi: 10.1109/GLOCOMW.2015.7414204.

[19] Pathuri, Lavanya & Satyanarayana, Penke & Ahmad, Afaq. (2019). Suitability of OFDM in 5G Waveform – A Review. Oriental journal of computer science and technology. 12. 66-75. 10.13005/ojcst12.03.01.
[20] H. Ochiai and H. Imai," On the distribution of the peak-to-average power ratio in OFDM signals," IEEE Trans. Commun., vol. 49, no. 2, pp. 282–289, Feb. 2001.
[21] P. Banelli, "Theoretical analysis and performance of OFDM signals in nonlinear fading channels," IEEE Trans. Wireless Commun., vol. 2, no. 2, pp. 284–293, Mar. 2003.
[22] P. Sivakumar, S. Sangeetha and M. Rajaram, "PAPR reduction in OFDM for SC-FDMA channels," *2011 International Conference on Signal Processing, Communication, Computing and Networking Technologies*, Thuckafay, 2011, pp. 6-9, doi: 10.1109/ICSCCN.2011.6024504.
[23] Myung, Hyung & Lim, Junsung & Goodman, David. (2006). Single Carrier FDMA for Uplink Wireless Transmission. Vehicular Technology Magazine, IEEE. 1. 30 - 38. 10.1109/MVT.2006.307304.
[24] Berardinelli, Gilberto & Pedersen, Klaus & B. Sorensen, Troels & Mogensen, Preben. (2016). Generalized DFT-Spread-OFDM as 5G Waveform. IEEE Communications Magazine. 54. 99-105. 10.1109/MCOM.2016.1600313CM.
[25] T. Obara, K. Takeda and F. Adachi, "Performance analysis of single-carrier overlap FDE," *2010 IEEE International Conference on Communication Systems*, Singapore, 2010, pp. 446-450, doi: 10.1109/ICCS.2010.5686606.
[26] Agilent Technologies. "LTE and the Evolution to 4G Wireless: Design and Measurement Challenges". John Wiley & Sons, 2009
[27] A. Silva, R. Holakouei, D. Castanheira, A. Gameiro, R. Dinis, "A novel distributed power allocation scheme for coordinated multicell systems", *EURASIP Journal on Wireless Communications and Networking*, Vol. 30, No. 30, February, 2013.
[28] Litwin, Louis & Pugel, Michael. "The principles of OFDM". RF signal processing, 2001.
[29] S. Prashanth G, "Orthogonal frequency division multiplexing (ofdm) based uplink multiple access method over awgn and fading channels", *International Research Journal of Engineering and Technology (IRJET)*,
[30] vol. 06, no. 04, pp. 1611–1617, Apr. 2019.
[31] Lande, Sudhir & Gawali, Jyoti & Kharad, S.M.. (2015). Performance Evolution of SC-FDMA for Mobile Communication System. 416-420. 10.1109/CSNT.2015.177.
[32] Hyung, G. Myung, "SC-FDMA", Wikimedia Commons
[33] DSP Illustration. 2018. "The Cyclic Prefix for OFDM", website, Dec. 2020 https://dspillustrations.com/pages/posts/misc/the-cyclic-prefix-cp-in-ofdm.html
[34] 5G/NR – Frame Structure, website, Feb. 2021 https://www.sharetechnote.com/html/5G/5G_FrameStructure.html
[35] Lande, Sudhir & Gawali, Jyoti & Kharad, S.. (2016). Performance Evolution of SC-FDMA for Mobile Communication System. International Journal of Future Generation Communication and Networking. 9. 231-242. 10.14257/ijfgcn.2016.9.2.24.
[36] A. Silva and A. Gameiro. Multiple antenna systems. Technical report, University of Aveiro: Comunicações sem fios lecture, 2019.
[37] Kong, Ning. (2009). Performance Comparison Among Conventional Selection Combining, Optimum Selection Combining and Maximal Ratio Combining. 1 - 6. 10.1109/ICC.2009.5199319.

[38] Milleth, J & Giridhar, K. & Jalihal, Devendra. (2015). Open-Loop and Closed-Loop Transmit Diversity Techniques—Overview and New Results. IETE Journal of Research. 51. 223-234. 10.1080/03772063.2005.11416398.
[39] Elzinati, Masoud, “Space-time Block Coding for Wireless Communications”, August 2008
[40] Vahid Tarokh; Nambi Seshadri & A. R. Calderbank (March 1998). "Space–time codes for high data rate wireless communication: Performance analysis and code construction". *IEEE Transactions on Information Theory*. **44** (2): 744–765.
[41] S.M. Alamouti (October 1998). "A simple transmit diversity technique for wireless communications". IEEE Journal on Selected Areas in Communications. 16 (8): 1451–1458
[42] Clerckx, Bruno & Oestges, Claude, “Mimo Wireless Networks (Second Edition)”, pages 385-418, Academic Press, 2013
[43] Jae Moung Kim, Sung Hwan Sohn, Ning Han, Seungwon Choi, Chiyoung Ahn, Gyeonghua Hong, & Yusuk Yun, “Chapter 16 - Cognitive Radio in Multiple-Antenna Systems”, “Cognitive Radio Technology (Second Edition)”, Academic Press, 2009,
[44] Waliullah, G. M. & Bala, Diponkor & Hena, Mst & Abdullah, Md & Hossain, Mohammad. (2020). Performance Analysis of Zero Forcing and MMSE Equalizer on MIMO System in Wireless Channel. 8. 19-25.
[45] A. Klein, G. K. Kaleh & P. W. Baier, "Zero forcing and minimum mean-square-error equalization for multiuser detection in code-division multiple-access channels," in *IEEE Transactions on Vehicular Technology*, vol. 45, no. 2, pp. 276-287, May 1996, doi: 10.1109/25.492851.
[46] García, M., Oberli, C. Intercarrier Interference in OFDM: A General Model for Transmissions in Mobile Environments with Imperfect Synchronization. *J Wireless Com Network* **2009,** 786040 (2009). https://doi.org/10.1155/2009/786040
[47] Silva, A., Assunção, J., Dinis, R. *et al.* Performance evaluation of IB-DFE-based strategies for SC-FDMA systems. *J Wireless Com Network* **2013,** 292 (2013). https://doi.org/10.1186/1687-1499-2013-292
[48] Kuhn, H, W & Tucker, (1951), “Nonlinear programming”. Proceedings of 2nd Berkeley Symposium. Berkeley: University of California Press, pages 481-492
[49] W. Karush (1939), “Minima of Functions of Several Variables with Inequalities as Side Constraints (M.Sc. thesis). Dept. of Mathematics, University of Chicago
[50] Dinis, R., Silva, P. and Gusmão, A. (2007), IB-DFE receivers with space diversity for CP-assisted DS-CDMA and MC-CDMA systems. Eur. Trans. Telecomm., 18: 791-802. https://doi.org/10.1002/ett.1238
[51] Ribeiro, F.C. & Guerreiro, João & Dinis, Rui & Cercas, Francisco & Jayakody, Dush Nalin. (2019). Multi-user detection for the downlink of NOMA systems with multi-antenna schemes and power-efficient amplifiers. Physical Communication. 33. 10.1016/j.phycom.2019.01.003.
[52] D. Castanheira, A. Silva, R. Dinis and A. Gameiro, "Efficient transmitter and receiver designs for SC-FDMA based heterogeneous networks," IEEE Trans. on Commun., vol. 63, no. 7, pp. 2500-2510, May 2015.
[53] A. A. Zaidi, R. Baldemair, H. Tullberg, H. Bjorkegren, L. Sundstrom, J. Medbo, C. Kilinc, and I. Da Silva, “Waveform and numerology to support 5G services and requirements, “, Ericsson Research